Traffic Through the *Trans*-Golgi Network and the Endosomal System Requires Collaboration Between Exomer and Clathrin Adaptors in Fission Yeast

Marta Hoya,* Francisco Yanguas,* Sandra Moro,* Cristina Prescianotto-Baschong,† Cristina Doncel,* Nagore de León,*,[1] M.-Ángeles Curto,* Anne Spang,† and M.-Henar Valdivieso*,[2]

*Department of Microbiology and Genetics, Institute of Functional Biology and Genomics (IBFG), University of Salamanca, Consejo Superior de Investigaciones Científicas (CSIC), 37007, Spain and †Biozentrum, University of Basel, CH-4056, Switzerland

ORCID ID: 0000-0002-6857-7493 (M.-H.V.)

ABSTRACT Despite its biological and medical relevance, traffic from the Golgi to the plasma membrane (PM) is one of the least understood steps of secretion. Exomer is a protein complex that mediates the trafficking of certain cargoes from the *trans*-Golgi network/early endosomes to the PM in budding yeast. Here, we show that in *Schizosaccharomyces pombe* the Cfr1 and Bch1 proteins constitute the simplest form of an exomer. Cfr1 co-immunoprecipitates with Assembly Polypeptide adaptor 1 (AP-1), AP-2, and Golgi-localized, gamma-adaptin ear domain homology, ARF-binding (GGA) subunits, and *cfr1*$^+$ interacts genetically with AP-1 and GGA genes. Exomer-defective cells exhibit multiple mild defects, including alterations in the morphology of Golgi stacks and the distribution of the synaptobrevin-like Syb1 protein, carboxypeptidase missorting, and stress sensitivity. *S. pombe apm1*Δ cells exhibit a defect in trafficking through the early endosomes that is severely aggravated in the absence of exomer. *apm1*Δ *cfr1*Δ cells exhibit a dramatic disorganization of intracellular compartments, including massive accumulation of electron-dense tubulovesicular structures. While the *trans*-Golgi network/early endosomes are severely disorganized in the *apm1*Δ *cfr1*Δ strain, *gga21*Δ *gga22*Δ *cfr1*Δ cells exhibit a significant disturbance of the prevacuolar/vacuolar compartments. Our findings show that exomer collaborates with clathrin adaptors in trafficking through diverse cellular compartments, and that this collaboration is important to maintain their integrity. These results indicate that the effect of eliminating exomer is more pervasive than that described to date, and suggest that exomer complexes might participate in diverse steps of vesicle transport in other organisms.

KEYWORDS clathrin adaptors; Golgi; endosomes; exomer; yeast

THE Golgi is a sorting node from where proteins are delivered to their final destinations following a retrograde route to the endoplasmic reticulum, or anterograde routes to the cell surface and to the vacuoles through the endosomal system. Additionally, there is direct traffic from the Golgi to the vacuoles. Different coats and adaptors facilitate trafficking between cell compartments (Lemmon and Traub 2000; De Matteis and Luini 2008; Anitei and Hoflack 2011; Barlowe and Miller 2013; Guo *et al.* 2014). Trafficking from the Golgi to the plasma membrane (PM) is less well-understood than other protein transport processes, such as trafficking from the endoplasmic reticulum to the Golgi or endocytosis (Spang 2015). It is known that a variety of membranous carriers transport different proteins from the Golgi to specialized domains of the PM (De Matteis and Luini 2008). While clathrin and the Assembly Polypeptide adaptor 1 (AP-1) are required for the packaging of some cargoes into carriers, other coats and adaptors participate in cargo sorting. Furthermore, in many cases, it has not been determined whether carriers bear specific receptors, adaptors, or coats (De Matteis and Luini 2008; Wakana *et al.* 2012; Bonifacino 2014; Spang 2015). Alterations in Golgi function and protein secretion are associated with human disease (Tang 2009; Bexiga and Simpson 2013). Therefore, the characterization of protein complexes acting in protein trafficking from the Golgi to the cell surface is of considerable biological and medical relevance.

doi: 10.1534/genetics.116.193458
Manuscript received July 5, 2016; accepted for publication December 9, 2016; published Early Online December 14, 2016.
Supplemental material is available online at www.genetics.org/lookup/suppl/doi:10.1534/genetics.116.193458/-/DC1.
[1]Present address: Department of Zoology, University of Oxford, OX1 3PS, UK.
[2]Corresponding author: Lab P1.1, Edificio Instituto de Biología Funcional y Genómica (IBFG), Calle Zacarías González 2, 37007 Salamanca, Spain. E-mail: henar@usal.es

Clathrin and AP-1 participate in the traffic between the *trans*-Golgi network (TGN) and early endosomes (EEs), and contribute to the retention of some proteins, including the *Saccharomyces cerevisiae* chitin synthase Chs3 and murine mannose-6-phosphate receptor, at the TGN (Meyer *et al.* 2000; Valdivia *et al.* 2002). The clathrin adaptor AP-2 participates in clathrin-mediated endocytosis, delivering proteins from the PM to the EEs, from where proteins can be sorted to the PM and to the Golgi. Additionally, EEs maturate into late endosomes (LEs) that produce multivesicular bodies (MVBs), which fuse to the lysosomes (vacuoles in yeast) (Huotari and Helenius 2011). In yeast, the term prevacuolar compartment (PVC) includes the LEs and MVBs (Scott *et al.* 2014). Protein trafficking from the Golgi to the PVC requires the participation of GGA (Golgi-localized, Gamma-adaptin ear domain homology, ARF-binding) adaptors. Although GGAs mediate transport from the TGN to the PVC, both in mammals and budding yeast, they also interact and colocalize with EE proteins. Furthermore, budding yeast GGAs contribute to Chs3 cycling between the TGN and EEs, and participate in the cycling of the synaptobrevin-related protein Snc1 between the PM and EEs (Black and Pelham 2000; Doray *et al.* 2002; Copic *et al.* 2007; Hirst *et al.* 2012). Direct trafficking from the Golgi to the vacuoles requires AP-3.

Exomer mediates the transport of a subset of transmembrane cargoes from the TGN/EEs to the PM in *S. cerevisiae* (Santos and Snyder 1997, 2003; Ziman *et al.* 1998; Barfield *et al.* 2009; Ritz *et al.* 2014). It is a heterotetramer consisting of any two ChAPs (Chs5p-Arf1p-binding Proteins; Bch1, Bud7, Chs6, and Bch2) and two copies of the scaffold Chs5 (Sanchatjate and Schekman 2006; Trautwein *et al.* 2006; Wang *et al.* 2006; Paczkowski and Fromme 2014; Huranova *et al.* 2016). The best-characterized role of exomer is Chs3 trafficking from the Golgi to the PM. In exomer-deficient mutants, Chs3 is retained in an intracellular compartment that exhibits characteristics of TGN and EEs (Santos and Snyder 1997; Ziman *et al.* 1998; Sanchatjate and Schekman 2006; Trautwein *et al.* 2006). As a consequence, cells are defective in the synthesis of the cell wall, the fungal counterpart of the extracellular matrix. AP-1 disruption in exomer mutants allows Chs3 rerouting to the PM through an alternative pathway, showing a functional relationship between exomer and this clathrin adaptor for chitin synthesis (Valdivia *et al.* 2002).

Proteins similar to exomer subunits are present in fungi but not in Metazoa. Nevertheless, an in-depth analysis of exomer can help to understand protein secretion in higher eukaryotes because it interacts with conserved proteins involved in trafficking from the Golgi to the PM. Additionally, protein complexes with similar architecture might exist in other organisms. While *S. cerevisiae* has four ChAPs, other organisms have either two or a single ChAP (Roncero *et al.* 2016). With the aim of gaining additional information about exomer, we have studied it in the distantly-related yeast *Schizosaccharomyces pombe*, which lacks chitin and bears a Chs5 homolog (Cfr1, Cartagena-Lirola *et al.* 2006) and one ChAP (Bch1). We have found that Cfr1 and Bch1 form a complex that localizes at the TGN in an Arf1-dependent manner, as exomer does. This rudimentary exomer exhibits interactions with the AP-1, AP-2, and the GGA clathrin adaptors. Collaboration between exomer and AP-1 and between exomer and the GGAs is required for trafficking to the cell surface and to the vacuoles, respectively, and to maintain the integrity of the endosomal/vacuolar system. Our results show that exomer function is wider and more general than previously reported.

Materials and Methods

Strains and growth conditions

Techniques for *S. pombe* growth and manipulation have been previously described (Moreno *et al.* 1991; PombeNet: www-bc*f*.usc.edu/∼forsburg/index.html). Unless otherwise stated, cells were grown in rich medium (YES: 0.5% yeast extract, 3% glucose, 225 mg/l adenine, histidine, leucine, uracil, and lysine hydrochloride, and 2% agar), incubated at 28° overnight, then reinoculated in fresh medium and incubated at 32° for 3 hr. Caspofungin (the active compound in Cancidas) was used at different concentrations from a 10 mg/ml stock in DMSO. For drop-test analyses, 3×10^4 cells and serial 1:4 dilutions were spotted onto plates that were incubated at different temperatures.

Genetic methods

Molecular and genetic manipulations were according to Sambrook and Russell (2001). *bch1*Δ deletions were generated by replacing the gene ORF by the *KANMX6* and *NATMX6* selection markers from cassettes bearing 0.5 kb DNA sequences upstream and downstream from the ORF. The Green Fluorescent Protein (GFP) was introduced as a *Not*I-*Not*I DNA fragment at *Not*I sites created by site-directed mutagenesis, either immediately after the starting ATG or before the stop codon in *bch1*$^+$; these resulting constructs, in which the gene was under the control of its own promoter, were integrated at the *leu1*$^+$ locus. Both constructs had the same localization in all strains analyzed. Complementation of KCl sensitivity showed that the tagged Cfr1 and Bch1 proteins were functional (data not shown). The *cfr1*$^+$-tagged versions always bore the tag before the stop codon (Cartagena-Lirola *et al.* 2006). Gga22-GFP was constructed by PCR amplification of 0.5 kb DNA fragments upstream and downstream to the ORF from genomic DNA, and PCR amplification of the ORF from a complementary DNA (cDNA) library. These fragments and GFP were ligated into a KS+ vector bearing the *ura4*$^+$ gene as a selectable marker; the plasmid was integrated into the *gga22*$^+$ locus. The FYVE(EEA1) phosphatidylinositol-3-phosphate-binding probe was PCR-amplified from plasmid pRS424GFP-FYVE(EEA1) (#36096 Addgene; Burd and Emr 1998), ligated to the C-terminal end of mCherry, and cloned under the control of the *nda2*$^+$ promoter and terminator into the pINTHA vector (Fennessy *et al.* 2014). The construct was transformed into the hph.171K strain (Fennessy *et al.* 2014; Yeast Genome Resource Center #FY23692). The accuracy of

the constructions was assessed by DNA sequencing, and correct integration by PCR. Genetic crosses and selection of the characters of interest by random spore analysis (Moreno *et al.* 1991) were used to combine different traits.

Cell wall analysis and β-glucan synthase activity

Cell wall composition and β-glucan synthase activity were analyzed as previously described (Perez and Ribas 2004; Sharifmoghadam and Valdivieso 2009).

Protein methods

Western blots to detect soluble proteins were performed as described (Sharifmoghadam and Valdivieso 2009; de León *et al.* 2016). To detect membrane proteins, the cleared lysates were incubated in the presence of 1.6 M urea in a tube rotator for 16 hr at 4° and the proteins were denatured at 65° for 5 min. Primary antibodies were anti-GFP (JL8, 1:3000; BD Living Colors), anti-HA (12CA5, 1:5000; Roche), anti-α tubulin (clone B-5-1-2, 1:10,000; Sigma [Sigma Chemical], St. Louis, MO), anti-Cpy1 (clone 10A5B5, 1:100; Invitrogen, Carlsbad, CA), anti-Pep12 (clone 2C4G4, 1:500; Life Technologies), polyclonal anti-DsRed (1:1000; Clontech, #632496), polyclonal anti-Pma1 (Reyes *et al.* 2007, 1:10,000), and polyclonal anti-human ATP6V1B2 (1:500; ABNOVA #H00000526-D01P, which recognizes fission yeast Vma2; Sanchez-Mir *et al.* 2014). Horseradish peroxidase-conjugated anti-mouse (1:10,000; BIORAD #170-6515) and anti-rabbit (1:10,000; clone RG-96, Sigma [Sigma Chemical]) secondary antibodies were used. Colony dot-blots were performed from colonies incubated at 28° using an antibody raised against *S. cerevisiae* Cpy1, as described (de León *et al.* 2013). For co-immunoprecipitations, cells lysates were obtained in the presence of 0.5% IGEPAL CA-630 (NP-40) and immunoprecipitations were performed in the presence of 0.25% IGEPAL CA-630 and 1% Triton X-100, as described (Sharifmoghadam and Valdivieso 2009).

Subcellular fractionation by sucrose density gradient centrifugation

Mini-step sucrose gradients were designed to separate TGN/EE fractions from PVC/vacuole fractions. Cells from 40-ml cell cultures at an OD_{600} 1.0 were collected by centrifugation at 3000 rpm for 3 min, washed with 1 ml STOP buffer (10 mM EDTA, 154 mM NaCl, 10 mM NaF, and 10 mM NaN_3) and with 1 ml of 5 mM EDTA/50 mM Tris pH 7.5, and resuspended in 3 ml of lysis buffer (20 mM Tris pH 7.2, 1 mM EDTA, 10% sucrose, and 17 μM GTP-γ-S with protease inhibitors). Cells were broken with cold glass beads (in a Fast-Prep 24; MP Biomedicals) in five 30-sec pulses at a 6.5 strength, with 5-min incubations on ice between the pulses. Extracts were recovered in a final volume of 5 ml of lysis buffer and cleared by centrifugation (5000 rpm for 5 min). Membranes were pelleted by centrifugation at 100,000 × *g* for 1 hr (using a 70 Ti rotor and a Beckman Optima LE-80 ultracentrifuge) and resuspended in 300 μl of 10% sucrose in HE buffer (20 mM HEPES, pH 7.2 and 1 mM EDTA). Aliquots (250 μl) of the extracts were layered on top of a mini-step sucrose gradient made as follows: 0.25 ml 55%, 0.5 ml 50%, 0.5 ml 45%, 0.75 ml 40%, 0.75 ml 37.5%, 0.75 ml 35%, 0.5 ml 32.5%, and 0.25 ml 30% sucrose (w/v) in HE buffer. Gradients were centrifuged at 38,000 rpm for 20 hr using a SW55 rotor. Seventeen 0.25-ml fractions were manually collected from the top of the gradient, treated with urea as above, and denatured in Laemmli sample buffer for 20 min at 37°. Samples from fractions 3 to 16 (35 μl) were loaded in polyacrylamide gels and analyzed by western blot. Each gradient was performed six times.

Microscopy

Staining with Calcofluor (Blankophor, Bayern; 0.125 μg/ml final concentration), FM4-64 (SynaptoRed; Biotium), and CDCFDA (5[6]-Carboxy-2′,7′-dichlorofluorescein diacetate; Sigma Chemical) was performed as described (Sharifmoghadam and Valdivieso 2009; de León *et al.* 2013). For treatment with Brefeldin A (Sigma Chemical; 100 μg/ml from a stock at 5 mg/ml in ethanol), cells were incubated in the presence of the drug for 10 min at 30° before being photographed. Cells were treated with latrunculin A (100 μM from a 5 mM stock in DMSO; Sigma Chemical) at different times.

Images were captured with either a Leica DM RXA conventional fluorescence microscope, equipped with a Photometrics Sensys CCD camera (using the Qfish 2.3 program), or with an Olympus IX71 microscope equipped with a personal DeltaVision system (with a Photometrics CoolSnap HQ2 monochrome camera). In the latter case, stacks of z-series sections were acquired at 0.2-μm intervals. Images are either two-dimensional maximum intensity projections of the six z-series that corresponded to the middle of the cell, or medial planes, and were analyzed using deconvolution software from Applied Precision. For confocal live-cell imaging, a Spinning-Disk Olympus IX-81 microscope, equipped with a confocal CSUX1-A1 module (Yokogawa) and a EVOLVE de PHOTOMETRICS camera, was used. Images of three 0.150-μm z-sections were captured at 2-sec intervals along 100/200-point time-lapses. Images were processed with Adobe Photoshop, IMAGEJ (National Institutes of Health), or SOFTWORX DV software.

For electron microscopy, cells were prefixed in glutaraldehyde (EM Grade), treated with 2% potassium permanganate, dehydrated in ethanol, embedded in TAAB Spurr's Resin, and stained with uranyl acetate. Samples were cut using a Reichert-Jung Ultracut ultramicrotome. Images were captured on a Philips CM-100 microscope.

Statistical analyses

Results were evaluated statistically using ANOVA with a Dunnett *post hoc* test using SPSS Statistic 17.0 software. *P*-values for the significantly different results are indicated (* $P \leq 0.05$, ** $P \leq 0.01$, *** $P \leq 0.001$, and **** $P \leq 00001$; n.s., not significant).

Data availability

Strains constructed in this work are available upon request. The strains used are listed in Supplemental Material, Table S1.

Results

S. pombe has the simplest form of exomer

S. pombe is a model yeast whose cell wall is mainly composed of glucans instead of chitin, and lacks homologs to all of the known exomer cargoes: the Family 2 chitin synthase Chs3, Fus1, and Pin2 (Santos and Snyder 1997, 2003; Ziman *et al.* 1998; Barfield *et al.* 2009; Ritz *et al.* 2014; Roncero *et al.* 2016). In spite of this, *S. pombe* bears a gene similar to *CHS5* (named *cfr1*$^+$, after chs five related; Cartagena-Lirola *et al.* 2006). Similar to Chs5, the Cfr1 N-terminal end of the protein (the FBE module) is necessary and sufficient for protein localization at the TGN and for functionality (Martin-Garcia *et al.* 2011; Paczkowski *et al.* 2012). Furthermore, the Cfr1 FBE module localizes to the Golgi both in *S. pombe* and *S. cerevisiae*, confirming a degree of conservation between Cfr1 and Chs5 (Martin-Garcia *et al.* 2011). *S. cerevisiae* ChAPs give cargo specificity, contribute to the stabilization of the complex at the TGN membrane, and promote membrane vesiculation (Sanchatjate and Schekman 2006; Trautwein *et al.* 2006; Wang *et al.* 2006; Paczkowski *et al.* 2012; Rockenbauch *et al.* 2012; Paczkowski and Fromme 2014; Huranova *et al.* 2016). According to PomBase (www.pombase.org/), the ORF SPBC31F10.16 is the only *S. pombe* gene coding for a protein with sequence similarity to the ChAPs. We named this gene *bch1*$^+$ because Bch1 is a conserved ChAP (Sanchatjate and Schekman 2006; Trautwein *et al.* 2006; Roncero *et al.* 2016).

To determine whether Cfr1 and Bch1 formed a complex, and whether this complex exhibited exomer characteristics, the localization of Bch1-GFP was analyzed in a strain bearing a Cfr1-RFP fusion protein. As shown in Figure 1A, Cfr1 and Bch1 colocalized and were observed as 7–9 intracellular fluorescents dots per cell. Furthermore, when co-immunoprecipitation between Bch1-GFP and Cfr1-HA was performed, the Cfr1-tagged protein was observed in immunoprecipitates from the strain bearing both tagged proteins, but not from the control strains (Figure 1B). Although co-immunoprecipitation does not show direct interaction, this result is in agreement with recent data from a massive *S. pombe* two-hybrid analysis, where Cfr1-Bch1 interaction was detected (Vo *et al.* 2016). These results indicate that Cfr1 and Bch1 form part of the same complex.

Cfr1 partially colocalized with the α-1,2-galactosyltransferase Gma12 (Cartagena-Lirola *et al.* 2006). In this work, we used additional Golgi markers and a better microscope to obtain more detailed information regarding Cfr1 localization. We found that Cfr1 never colocalized with the early-Golgi marker Anp1 (Figure 1C), while 80% of the Cfr1-RFP dots colocalized with the GFP-tagged TGN marker Sec72 (a Sec7 ortholog). In fungi, EEs cannot be morphologically distinguished from the TGN but can be considered as its extension (Huotari and Helenius 2011). We investigated whether Cfr1 was only present in the TGN or also populated the EEs by analyzing colocalization of Cfr1-GFP and FM4-64 (Figure 1D), a lipophilic dye that enters the cell through the endocytic route. Data quantification using JaCoP (Just another Colocalization Plugin) from the ImageJ software indicated that 31% of the Cfr1-GFP dots colocalized with FM4-64, and that 27.5% of the FM4-64-stained endosomes colocalized with Cfr1-GFP dots, confirming the presence of exomer in endosomes.

We have previously shown that Brefeldin A disrupted Cfr1 localization at the Golgi (Cartagena-Lirola *et al.* 2006). However, in those experiments the drug was present in the culture for 2 hr. We wanted to confirm this result using a milder treatment. As shown in Figure 1E, both Cfr1 and Bch1 lost their TGN/EE localization after 10-min incubation in the presence of Brefeldin A; this result confirmed that Arf1-dependent activity promoted the recruitment of these proteins to the Golgi. Finally, the localization of each protein in the absence of the other was investigated; neither Cfr1-GFP nor Bch1-GFP was observed as discrete fluorescent dots in strains lacking the other exomer component (Figure 1F). Thus, the *S. pombe* exomer components are interdependent for localization at the TGN/EEs. Recent studies have shown that different ChAPs have particular properties, and that Bch1 contributes to the stabilization of Chs5 at the TGN more than the other ChAPs (Paczkowski and Fromme 2014; Huranova *et al.* 2016). It seems that in *S. pombe*, where there are no additional ChAPs, Bch1 may be essential to stabilize Cfr1 at the membranes.

Taken together, these results showed that *S. pombe* Cfr1 and Bch1 proteins exhibit the characteristics of an exomer complex.

There is functional interaction between exomer and clathrin adaptors

The best-characterized role of exomer is facilitating the transport of the Chitin synthase Chs3 from the TGN to the cell surface (Santos and Snyder 1997; Santos *et al.* 1997; Ziman *et al.* 1998). In *S. pombe*, the main structural cell wall components are glucans, and accordingly, we analyzed whether glucan synthesis was altered in exomer mutants. Genetic interaction between *cfr1*Δ and *cps1-191* was detected (Figure S1, *cps1-191* strain that bears a mutation in the β-glucan synthase *bgs1*$^+$; Liu *et al.* 2000), which suggested a defect in cell wall synthesis in *cfr1*Δ. However, β-glucan synthases (Bgs1, Bgs3, and Bgs4), and the α-glucan synthase (Ags1) were efficiently delivered to the PM in exomer mutants (Figure S1, Figure S2, and Figure S3). Thus, *S. pombe* exomer was not dedicated to the trafficking of glucan synthases. Interestingly, the *S. cerevisiae* β(1,3)-glucan synthase *FKS1* (a transmembrane protein that localizes in a polarized way at the cell growth sites) was properly delivered to the cell surface in the *chs5*Δ mutant (Figure S1), suggesting that glucan synthases might not be exomer cargoes. Similarly, other *S. pombe* proteins with a

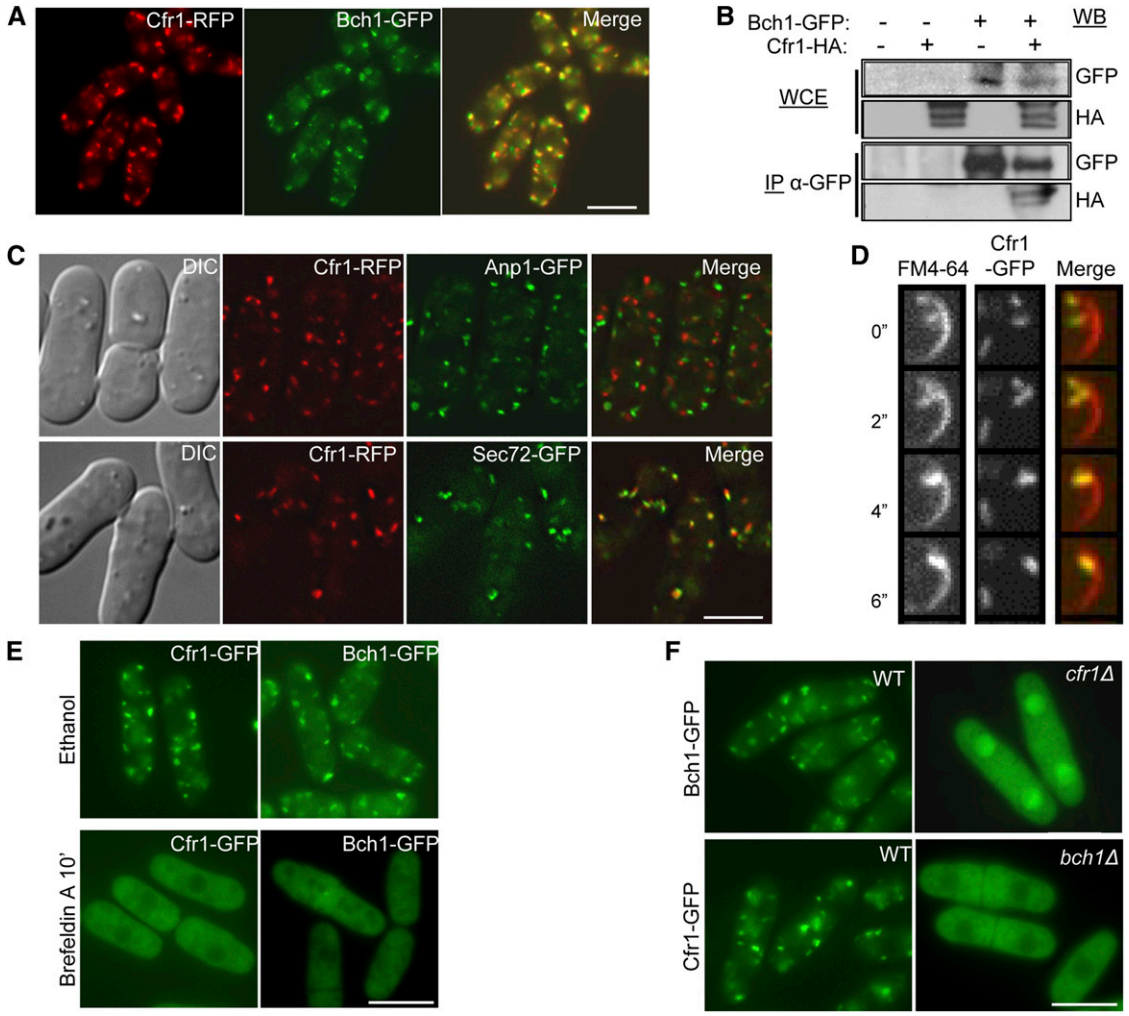

Figure 1 *S. pombe* Cfr1 and Bch1 proteins form a complex with exomer characteristics. (A) Cfr1 and Bch1 colocalize. (B) Cfr1 and Bch1 co-immunoprecipitate; cell extracts from an untagged strain and from strains carrying Bch1-GFP and/or Cfr1-HA were analyzed by western blot (WB) using anti-GFP or anti-HA monoclonal antibodies before (WCE, whole-cell extracts) or after immunoprecipitation (IP) with a polyclonal anti-GFP antibody. (C) Cells bearing the indicated fusion proteins were photographed with a DeltaVision deconvolution system. Differential interference contrast (DIC) and medial sections of the fluorescence images from cells bearing Cfr1-RFP (red fluorescent protein), the *cis*-Golgi marker Anp1-GFP, and the *trans*-Golgi marker Sec72-GFP are shown. (D) Cells bearing Cfr1-GFP were counterstained with FM4-64 and photographed under a spinning-disk confocal microscope after the indicated times. Images are medial sections of a cell tip. (E) Cells bearing Cfr1-GFP and Bch1-GFP were incubated in the presence of ethanol (solvent) or the Arf1 inhibitor Brefeldin A. (F) Cfr1 and Bch1 depend on each other for their localization at the TGN/EEs. Unless otherwise stated, cells were photographed under a conventional fluorescence microscope. Bar, 10 μm.

direct role in cell wall synthesis (Gas1 and Gas2 transglycosylases), glucan synthesis regulators (Rho1 and Cfh3), and proteins involved in protein trafficking whose delocalization might account for this defect (Apm1 and Clc1), were properly localized (Figure S1). Thus, contrary to the situation found in budding yeast, *S. pombe* exomer does not play a major role in cell wall synthesis. Additionally, the distribution of some PM proteins unrelated to cell wall synthesis, such as the chitin synthase-related protein Chs2 (Martin-Garcia *et al.* 2003) and the ATPase Pma1, was also unperturbed in the *cfr1*Δ mutant (Figure S1).

In *S. cerevisiae apm1*Δ deletion suppresses *chs6*Δ resistance to Calcofluor because, in the absence of AP-1 and exomer, Chs3 is delivered to the cell surface through an alternative pathway (Valdivia *et al.* 2002). In the *S. pombe apm1*Δ mutant, defective in the AP-1 μ subunit, the transport of the β(1,3)-glucan synthase Bgs1 is defective such that part of the protein accumulates in endosomes (Yu *et al.* 2012). Accordingly, we analyzed whether exomer and AP-1 played opposite roles in the trafficking of glucan synthases in fission yeast, and whether exomer deletion would allow these enzymes to reach the PM in the *apm1*Δ strain. *apm1*Δ is sensitive to temperature and to the glucan synthase inhibitor micafungin (Kita *et al.* 2004). Surprisingly, we found synthetic growth defects in *apm1*Δ *cfr1*Δ strains in YES medium (Figure 2A), and in the presence of the β(1,3)-glucan synthase inhibitor Caspofungin (Figure 2B). These results showed genetic interaction between *cfr1*$^+$ and *apm1*$^+$, and

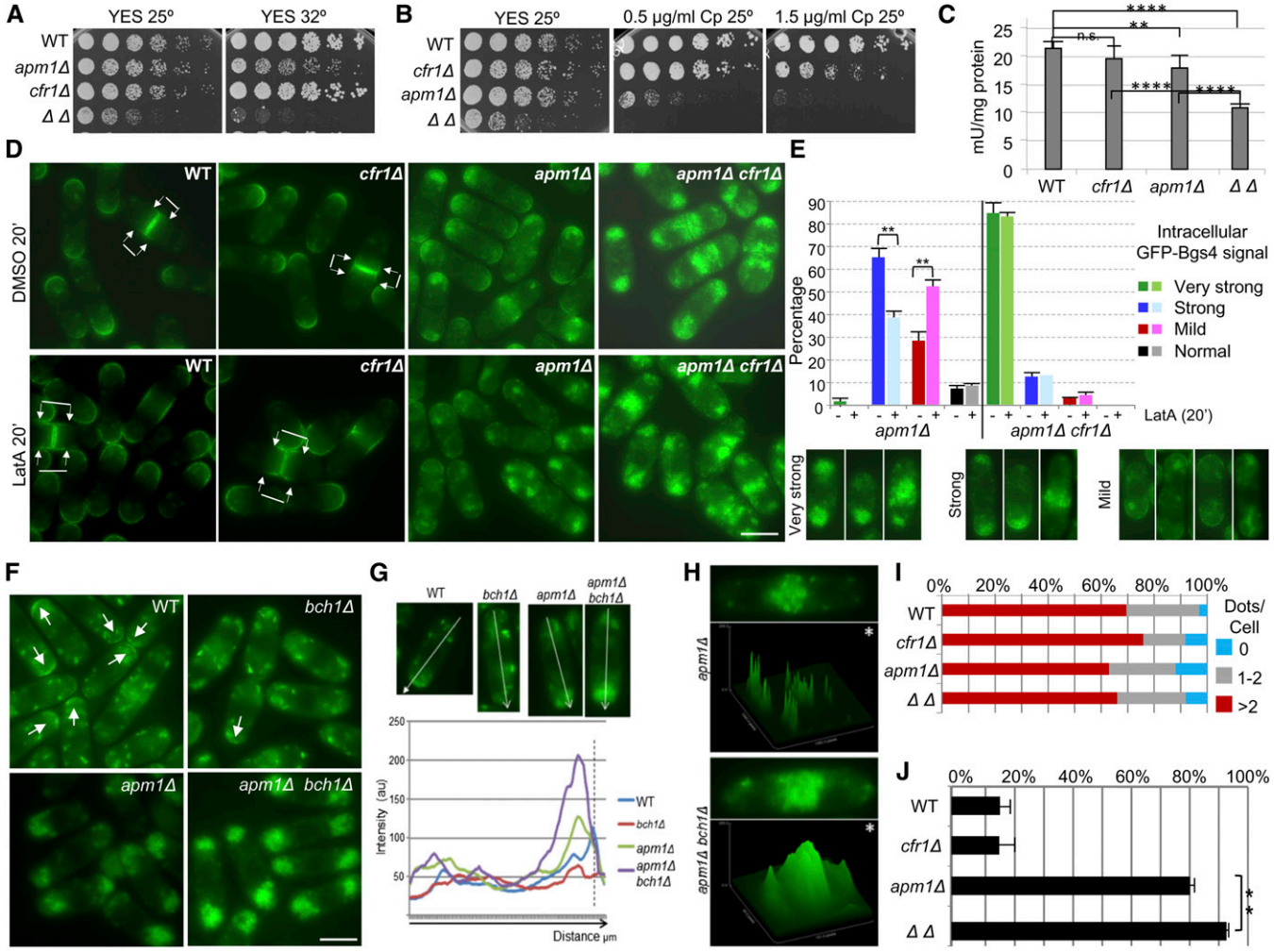

Figure 2 Functional interaction between exomer and AP-1. (A) Cells were spotted onto YES plates (0.5% yeast extract, 3% glucose, 225 mg/l adenine, histidine, leucine, uracil, and lysine hydrochloride, and 2% agar) and incubated at the indicated temperature for 2–5 days. (B) The indicated strains were spotted onto YES and YES with Caspofungin (Cp) plates and incubated at 25° for 5 days. (C) Cells lacking both exomer and AP-1 exhibit a severe reduction in β(1,3)-glucan synthase activity. Activity was estimated in membrane extracts from cells incubated in YES with sorbitol at 28°. The experiment was performed a minimum of five times with duplicates; the means, SD, and statistical significance of the differences are shown. (D) Cells bearing GFP-Bgs4 were treated with DMSO (solvent) or with Latrunculin A (LatA) for 20 min and photographed. Arrows delimit the plasma membrane region, proximal to the cell division site, where GFP fluorescence can be observed. (E) Percentage of cells exhibiting different degrees of intracellular GFP-Bgs4 fluorescence in cells treated or not with Latrunculin A (upper panel). Lower panels show micrographs of representative cells belonging to each cell type scored. (F) GFP-Syb1 localization is altered in the absence of exomer and Apm1. Arrows denote GFP fluorescence at the surface of cell poles. (G) Representative linescans of cells from the indicated strains performed to evaluate GFP-Syb1 fluorescence. The direction of the lines is indicated in the upper panels, and the lower panel shows the quantification of relative fluorescence intensity along the lines. The perpendicular dashed line indicates the position of cell surface. (H) Micrographs and the corresponding fluorescence surface plots (panels denoted by asterisks) of *apm1*Δ and *apm1*Δ *cfr1*Δ septating cells. (I) Percentage of cells with the indicated number of Cherry-FYVE(EEA1) dots, which were scored from micrographs. For each strain, a minimum of 300 cells were analyzed. (J) Percentage of cells in which all vacuoles had a diameter smaller than 0.75 µm. Cells were stained with CDCFDA and photographed. Vacuole diameter was scored from the photographs in a minimum of 25 cells. In (D–J) cells were incubated at 32° and photographed under a conventional fluorescence microscope. Bar, 10 µm. WT, wild-type.

suggested that exomer and AP-1 cooperate in a common functional pathway related, at least in part, with cell wall synthesis. To confirm this issue, the β(1,3)-glucan synthase activity was evaluated in membrane extracts from the wild-type (WT), *cfr1*Δ, *apm1*Δ, and *cfr1*Δ *apm1*Δ strains. The activity in the *apm1*Δ extracts was significantly lower than that in the WT extracts (Figure 2C), and it was further reduced in the double-mutant, confirming a collaboration between exomer and AP-1 for the regulation of β(1,3)-glucan synthesis. The simplest explanation for this result would be that, in fission yeast, AP-1 and exomer collaborate for the delivery of glucan synthases from the TGN/EEs to the PM. In agreement with this hypothesis, we detected a prominent accumulation of all glucan synthases inside the *apm1*Δ cells, which was enhanced in the *apm1*Δ *cfr1*Δ mutant (Figure 2, D and E, Figure S2, and Figure S3); conversely, the signal of glucan synthases at the cell surface was weaker in *apm1*Δ than in WT cells, and even weaker in the double-mutant. To better

characterize the defect in the trafficking of glucan synthases, their level was estimated by western blot in the WT, *apm1*Δ, *cfr1*Δ, and *apm1*Δ *cfr1*Δ strains. This experiment revealed that the amount of each synthase was similar in all of these strains (Figure S2), suggesting that their trafficking between the TGN/EEs and the vacuole was not hampered in the mutants. All these results established a correlation between the growth defects in the presence of Caspofungin and at high temperature, the reduction in β(1,3)-glucan synthase activity, and a defect in the trafficking of glucan synthases to the PM, and showed that exomer and AP-1 collaborate in this traffic.

Next, WT, *apm1*Δ, *cfr1*Δ, and *apm1*Δ *cfr1*Δ strains bearing GFP-Bgs4 were treated with latrunculin A, a drug that inhibits endocytosis. As shown in Figure 2D, after a 20-min incubation of the WT and *cfr1*Δ strains in the presence of latrunculin A, GFP-Bgs4 fluorescence extended from the cell tips and equator along the lateral PM (denoted by arrows). This result showed that endocytosis plays a role in limiting the localization of Bgs4 to the sites of polarized growth, as described for other PM proteins (Valdez-Taubas and Pelham 2003). In the *apm1*Δ strain, the level of intracellular GFP signal was partially reduced after latrunculin A was added to the culture (Figure 2, D and E), showing that the Bgs4 protein that accumulated inside the cells was, at least in part, of endocytic origin. In the *apm1*Δ *cfr1*Δ double-mutant, the intracellular accumulation of Bgs4 was not resolved by the presence of the drug (Figure 2, D and E); longer latrunculin A treatments did not reduce intracellular Bgs4 accumulation in this strain (Figure S3). The culture OD_{600} increased along the experiment, showing that cells were alive (data not shown). These results suggested that the compartments where Bgs4 was retained in *apm1*Δ and *apm1*Δ *cfr1*Δ mutants had different characteristics.

To understand whether the defect in Bgs4 trafficking was specific, or was related a general defect in the trafficking machinery in the absence of AP-1 and exomer, the distribution of Syb1 (the v-SNARE that mediates fusion of Golgi-derived vesicles to the PM) was analyzed in WT, *bch1*Δ, *apm1*Δ, and *apm1*Δ *bch1*Δ strains; *bch1*Δ strains were used as exomer mutants because *cfr1*Δ strains bearing GFP-Syb1 could not be obtained. As described (Edamatsu and Toyoshima 2003), in the WT strain, most of GFP-Syb1 was observed in endosomes, while a weak signal was observed at the cell poles and equator (Figure 2F). In the *bch1*Δ strain, the intracellular distribution of Syb1 was similar to that of the control while the signal at the cell surface was weaker, as confirmed by linescan quantification using ImageJ software (Figure 2G). According to data quantification, Syb1 was detected at the cell surface in 82% of the WT cells and in 36% of the *bch1*Δ cells. These results indicated that Syb1 recycling between the TGN/EEs and the PM was altered in the absence of exomer. As described (Kita *et al.* 2004; Yu *et al.* 2012), a strong accumulation of GFP-Syb1 was observed inside *apm1*Δ cells, while no signal was detected at the cell surface (Figure 2F). This result was confirmed by linescan analysis (Figure 2G). In the double *apm1*Δ *bch1*Δ mutant, intracellular Syb1 accumulation was more severe than in the single *apm1*Δ mutant (Figure 2, F and G). Surface plots performed to evaluate the intensity of GFP-Syb1 fluorescence at the midzone of septating *apm1*Δ and *apm1*Δ *cfr1*Δ cells confirmed that the signal was more intense in the double- than in the single-mutant (Figure 2H). These results were in agreement with the hypothesis that trafficking through the TGN/EEs was strongly affected in the absence of both AP-1 and exomer.

Since vacuoles in *apm1*Δ cells are small and defective (Kita *et al.* 2004), we investigated whether the PVC/vacuoles were altered in the absence of both AP-1 and exomer. To do so, the localization of a Cherry-FYVE(EEA1) probe was analyzed and surprisingly, in *S. pombe*, this probe colocalized with Pep12 in PVC/vacuole membranes (Figure S4). This probe is specific for PI3P because its fluorescent signal cannot be observed in *pik3*Δ/*vps34*Δ cells (Figure S4); therefore, its presence in the PVC/vacuole probably indicates a considerable concentration of PI3P in the membranes of these compartments *in S. pombe*. When cells were incubated at 32°, the fluorescence around the vacuole was weak, while the signal in the PVC dots was prominent (compare the WT control in Figure S4, A and D). We found that the pattern of FYVE(EEA1) localization was apparently similar in the WT, *cfr1*Δ, *apm1*Δ, and *apm1*Δ *cfr1*Δ strains (Figure 2I and Figure S4D), suggesting that the general organization of the PVC was not altered in the mutants. Regarding vacuoles, cell staining with CDCFDA (a vital dye for the vacuole lumen) revealed that vacuole size in WT and *cfr1*Δ strains was similar, with 15.3 ± 0.8% and 16.1 ± 1.2% cells where all the vacuoles were smaller than 0.75 μm. In *apm1*Δ cells, this value reached 79.1 ± 2.3%, and was as high as 91.7 ± 1.1% in the *apm1*Δ *cfr1*Δ strain (Figure 2J and Figure S4E).

All the results described above show that the absence of exomer enhanced *apm1*Δ defects, and strongly suggests that, in the double-mutant, intracellular compartments are altered.

The integrity of TGN, endosomes, and vacuoles requires collaboration between exomer and AP- 1

To obtain more detailed information about the possible alteration of organelles, cells were incubated at 32° and observed by transmission electron microscopy. The general appearance of WT and *cfr1*Δ cells was similar (Figure 3A). However, a detailed observation revealed that, in *cfr1*Δ cells, the Golgi had numerous stacks (micrographs b–e in the *cfr1*Δ panel in Figure 3B) that were engorged (micrograph b) or disorganized (micrographs d and e), something that was infrequent in the control strain (micrograph d in the WT panel). Thus, in the absence of exomer, Golgi organization was altered. *S. pombe* cells contain numerous small vacuoles that can appear as electron-dense or electron-translucent structures; the difference between both structures has not been analyzed in detail and authors denote both of them as vacuoles. There were no remarkable differences in the general appearance of the vacuolar system in the WT and *cfr1*Δ strains (denoted as

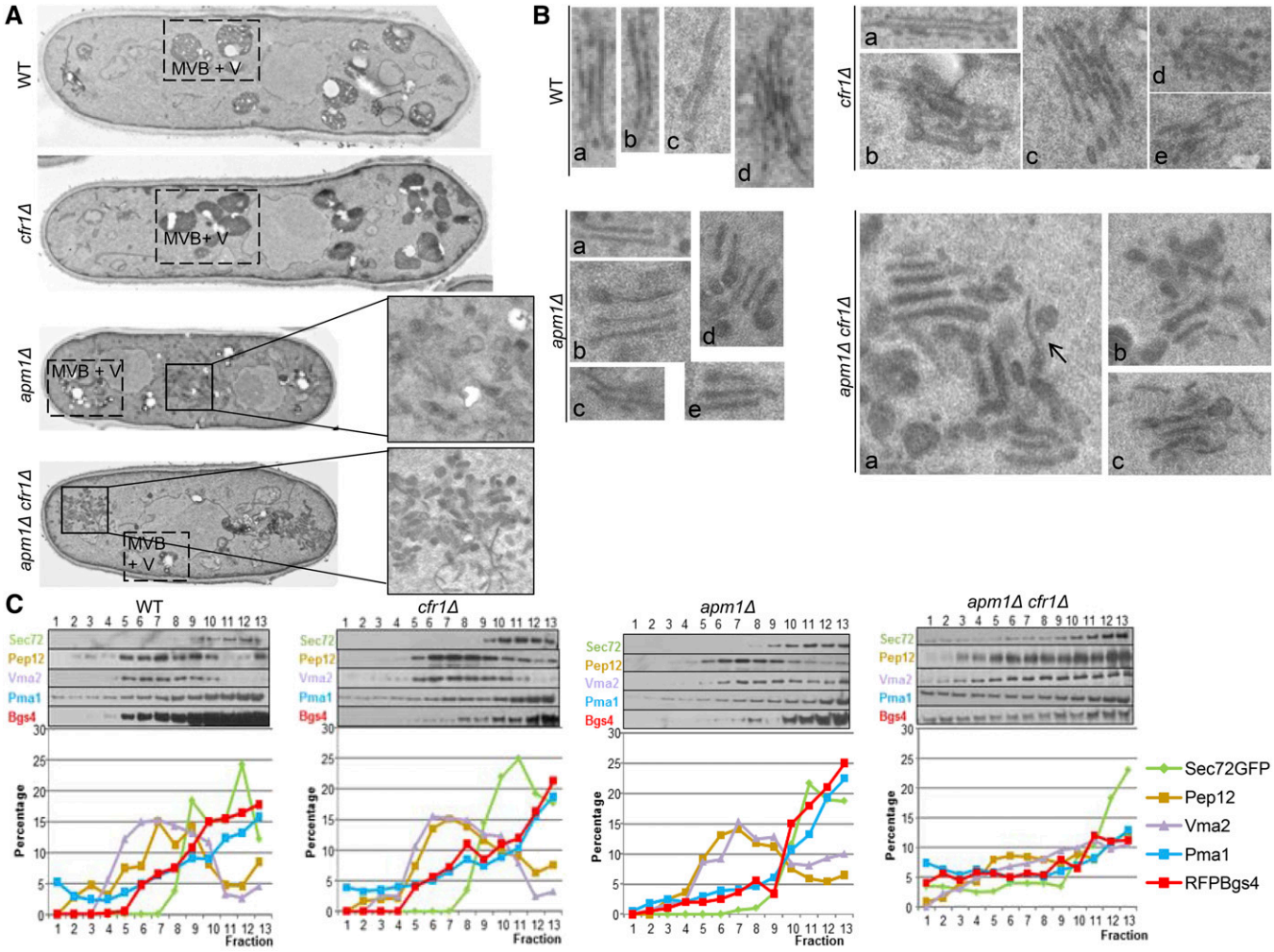

Figure 3 Exomer and AP-1 complexes collaborate to maintain the organization of the endosomal system. (A) Wild-type (WT), *cfr1*Δ, *apm1*Δ, and *apm1*Δ *cfr1*Δ cells were analyzed by electron microscopy. In all cases, MVB+V denotes multivesicular bodies and vacuoles. For *apm1*Δ and *apm1*Δ *cfr1*Δ cells, cell regions where accumulation of endomembranes could be observed have been enlarged. (B) Enlarged sections of micrographs from the same strains to allow better visualization of the Golgi apparatuses; panels denoted by lowercase letters correspond to different examples from the same strain. In the case of *apm1*Δ *cfr1*Δ, the arrow points to a tubulo-vesicular connection. (C) Cell extracts from the indicated strains bearing RFP-Bgs4 and Sec72-GFP fusion proteins were centrifuged to equilibrium on mini-step sucrose gradients. Fractions were collected from the lighter to the heavier ones and analyzed by western blot using anti-GFP (Sec72; TGN/EE), anti-Pep12 (PVC), anti-Vma2 (vacuole), anti-Pma1 (PM), and anti-RFP (Bgs4 and PM) antibodies (upper panels). For each protein and strain, the relative level in each fraction with respect to its total level was estimated (lower panels). In all cases, cells were incubated at 32°. EE, early endosomes; MVB, multivesicular body; PM, plasma membrane; PVC, prevacuolar compartment; RFP, red fluorescent protein; TGN, *trans*-Golgi network; V, vacuole.

MVB+V in Figure 3A). In *apm1*Δ, accumulation of amorphous membranous structures was observed inside half of the cells (Figure 3A. $n = 12$ imaged cells); this accumulation was never observed in the WT. Additionally, vacuoles were smaller than in the control strain. Finally, in this mutant, Golgi stacks exhibited swollen tips and were distant from each other (micrographs b and d in the *apm1*Δ panel in Figure 3B). Remarkably, in most of the *apm1*Δ *cfr1*Δ cells, there was a strong accumulation of electron-dense structures (Figure 3A) that appeared as tubules and vesicles (Figure 3, A and B) that were connected (arrow in the *apm1*Δ *cfr1*Δ panel a in Figure 3B). These structures, which were absent from the control and *cfr1*Δ strains and infrequent in the *apm1*Δ cells, were reminiscent of those described for the *apm1*Δ single-mutant after an 8-hr incubation at 36° (Kita *et al.* 2004). Golgi stacks were engorged and disorganized (Figure 3B). Thus, the absence of exomer seemed to enhance the disturbance in the TGN/EEs produced by the absence of AP-1. The general appearance of vacuoles in the *apm1*Δ *cfr1*Δ strain was similar to that of the *apm1*Δ single-mutant (Figure 3A).

Next, to obtain additional evidence supporting the hypothesis that the alteration of subcellular compartments is stronger in *apm1*Δ *cfr1*Δ than in *apm1*Δ, cell extracts from strains bearing RFP-Bgs4 and Sec72-GFP were subjected to subcellular fractionation in mini-step sucrose gradients. In the WT, *cfr1*Δ, and *apm1*Δ strains, Pep12 (PVC marker) and Vma2 (vacuole marker) largely cofractionated, forming a wide peak that occupied most of the central part of the gradient. PM markers (Bgs4

and Pma1) were detected in all of the fractions analyzed, with their concentrations increased from the lighter fractions to the heavier ones, and most of the protein cofractionating with the TGN/EE marker Sec72 (Figure 3C). Eliminating exomer in the *apm1*Δ strain had a dramatic effect on the distribution of some markers; thus, in the *apm1*Δ *cfr1*Δ mutant, the Pep12 and Vma2 fractions did not form clear peaks. Additionally, the distribution of PM markers was altered, with their level being more prominent in the lighter fractions of the gradient than in the control strains. As a consequence, in the double-mutant, the amount of these proteins did not exhibit the strong increase in the heaviest fractions observed in the rest of the strains. These results were in agreement with organelles being altered in the *apm1*Δ *cfr1*Δ strain, and showed that collaboration between exomer and AP-1 is relevant for their organization. This alteration would account for the severe trafficking and growth defects exhibited by this strain.

The integrity of the PVC/vacuole compartments requires collaboration between exomer and GGA adaptors

The enhancement of vacuole defects in the *apm1*Δ *cfr1*Δ strain could be an indirect consequence of the stronger alteration in the traffic through the TGN/EEs in the double-mutant. It was also possible that exomer mutants had a failure in trafficking from the TGN/EEs to the vacuoles that, when combined with the vacuolar defect in *apm1*Δ strain, would lead to a stronger defect in this step of trafficking. A standard assay to detect alterations in protein trafficking from the Golgi to the vacuole involves performing anti-Cpy1 dot-blot analyses to determine carboxypeptidase missorting to the cell surface. As shown in Figure 4A, the Cpy1 signal detected in the exterior of the colonies from the *cfr1*Δ, *bch1*Δ, and *cfr1*Δ *bch1*Δ strains was stronger than that of the WT control. Since cell lysis was not detected in the colonies by methylene blue staining, this result revealed a defect in Cpy1 trafficking in exomer mutants. This signal was specific, because it was stronger in a mutant missing exomer and the ESCRT0 subunit *vps27*$^+$ than in the corresponding single-mutants, and it was stronger in a strain lacking both GGA adaptors (named *gga21*$^+$ and *gga22*$^+$ in *S. pombe*) and exomer than in the double *gga21*Δ *gga22*Δ mutant. Nevertheless, Cpy1 missorting in exomer mutants was weaker than in a strain missing the *vps34/pik3*$^+$ phosphatidylinositol 3-kinase, suggesting that this defect was mild. These results reveal that exomer function is not restricted to the trafficking between TGN/EEs and the PM, as had been reported (Santos and Snyder 1997; Ziman *et al.* 1998; Sanchatjate and Schekman 2006; Trautwein *et al.* 2006; Wang *et al.* 2006), and suggest that it might have additional functions in vesicle trafficking.

Next, the existence of a relationship between exomer and GGAs was examined. GGAs are clathrin adaptors that facilitate the transport of certain cargoes between the TGN and PVC. According to drop-test analyses, the double *gga22*Δ *cfr1*Δ mutant exhibited a partial growth defect at low temperature (22°) and at high temperature (36°), a defect that was not detected in the corresponding single-mutants (Figure 4B). Interestingly, the *gga21*Δ *gga22*Δ strain was unable to grow at 22°, showing that both GGA proteins acted in parallel routes. The triple *gga21*Δ *gga22*Δ *cfr1*Δ mutant was unable to grow at 36°, a temperature at which the single- and double-mutants exhibited growth, suggesting that exomer might collaborate with these adaptors in some aspects of trafficking.

Several experiments were then performed to understand the nature of the relationship between exomer and GGAs. First, the distribution of the PVC marker FYVE(EEA1) was analyzed in several strains incubated at 32°. The number of FYVE dots was lower in the *gga21*Δ mutant than in the WT (Figure 4C). In the *gga21*Δ *gga22*Δ mutant, dot number was lower than that in the corresponding single-mutants, and it was further reduced in the *gga21*Δ *gga22*Δ *cfr1*Δ strain. In the triple-mutant, the existence of more than two dots was extremely infrequent, and most cells did not exhibit any dot. Dots in the triple-mutant were also less frequent than in the *gga22*Δ *cfr1*Δ double-mutant, which had fewer dots than the corresponding single-mutants (Figure 4C). These results showed that the simultaneous absence of exomer and both GGAs produced a significant alteration in the PVC. Quantifying the number of FYVE(EEA1) dots per cell is an indirect assay to analyze the PVC, and we could not know whether the *gga21*Δ *gga22*Δ *cfr1*Δ mutant had less/smaller PVCs than the single- and double-mutants, or whether its PVC membrane had less PI3P. Nevertheless, since this alteration was not observed in either *apm1*Δ or *apm1*Δ *cfr1*Δ strains, these results supported the hypothesis that the relationship between exomer and AP-1 is different from the relationship between exomer and GGAs. To complement these studies, CDCFDA staining was used to evaluate vacuole number and morphology in the same strains incubated under the same conditions. As shown in Figure 4D and Figure S5, vacuoles in the strain missing both GGAs were larger than in the rest of the strains, with the exception of the triple *gga21*Δ *gga22*Δ *cfr1*Δ strain, which exhibited the largest vacuoles.

Finally, cells incubated at 32° were analyzed by electron microscopy. In the *gga21*Δ *gga22*Δ strain, it was possible to observe exaggerated MVBs with numerous small intraluminal vesicles (Figure 4E). An accumulation of MVBs was also observed in the *gga21*Δ *gga22*Δ *cfr1*Δ triple-mutant, which additionally exhibited an accumulation of abnormal pleomorphic vacuoles. These results were in agreement with a functional collaboration between exomer and GGA adaptors relevant to maintain the integrity of the vacuolar system. Additionally, the fact that the defects in PVC/vacuoles in *apm1*Δ *cfr1*Δ and *gga21*Δ *gga22*Δ *cfr1*Δ strains were different (Figure S6) strongly suggests that the defect in the latter strain was not an indirect consequence of alterations in the traffic through the TGN/EEs.

Nevertheless, since GGA adaptors have been proposed to be functionally related to AP-1 in metazoa and budding yeast, the distribution of GFP-Syb1 was compared in the same strains. In the single *gga21*Δ and *gga22*Δ mutants, cells exhibited 8.5 ± 1.2 intracellular fluorescent dots ($n \geq 10$ cells) whose distribution was similar to that of the WT

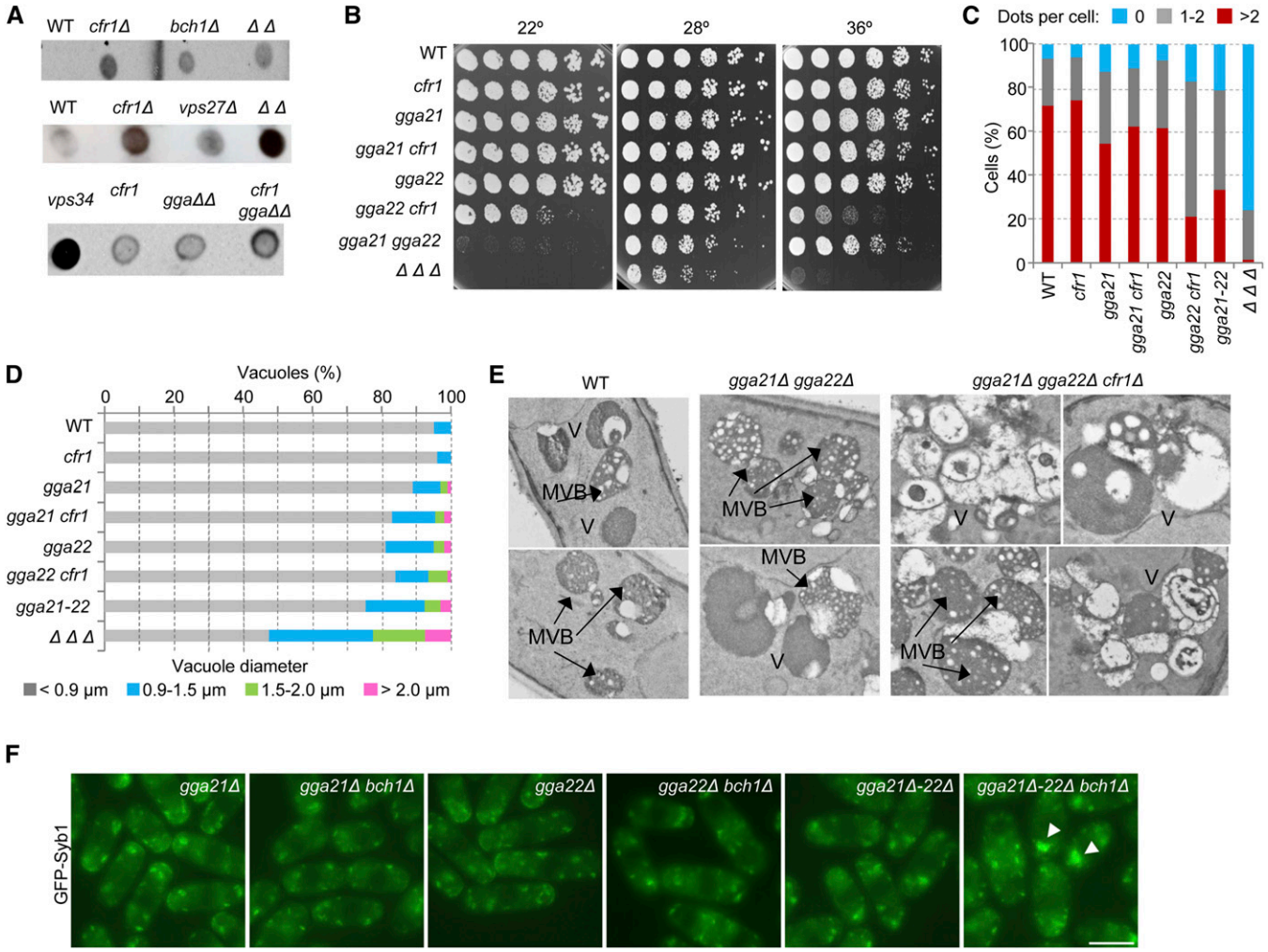

Figure 4 Exomer and GGA adaptors collaborate to maintain the organization of the prevacuolar/vacuolar system. (A) Nitrocellulose membranes, where colonies from the indicated strains had grown at 28°, were analyzed by dot-blot with anti-Cpy1. (B) Cells from the indicated strains were spotted onto YES and incubated at 22° for 7 days, at 28° for 3 days, and at 36° for 2 days. (C) The percentage of cells exhibiting the indicated number of FYVE(EEA1) dots per cells is shown. Dots were scored from photographs in a minimum of 300 cells. (D) Percentage of vacuoles with the indicated diameters. Cells were stained with CDCFDA and photographed. Vacuole diameter was estimated with ImageJ software from the photographs. For each strain, the vacuoles in a minimum of 25 cells were scored. (E) Electron microscopy of the vacuolar system in different strains. Two examples of wild-type and *gga21*Δ *gga22*Δ cells and four examples of *gga21*Δ *gga22*Δ *cfr1*Δ cells are shown. (F) GFP-Syb1 distribution. Arrowheads denote fluorescence accumulation inside the cells. Bar, 10 μm. In (C–F), cells were incubated at 32°. In (C), (D), and (F) cells were photographed under a conventional fluorescence microscope. GGA, Golgi-localized, gamma-adaptin ear domain homology, ARF-binding; MVB, multivesicular body; WT, wild-type; YES, 0.5% yeast extract, 3% glucose, 225 mg/l adenine, histidine, leucine, uracil, and lysine hydrochloride, and 2% agar.

control, and a signal at the cell surface of active growth sites (Figure 2F and Figure 4F). In double-mutants lacking one GGA and Bch1, Syb1 distribution was similar to that observed in the *bch1*Δ mutant, with the fluorescent signal being readily detected in intracellular dots (8.1 ± 1.9 dots per cell) but barely detected at the cell surface. In the *gga21*Δ *gga22*Δ strain, there were 9.9 ± 2.2 intracellular fluorescent dots per cell and, as described for the *S. cerevisiae gga1*Δ *gga2*Δ strain (Black and Pelham 2000), the v-SNARE could not be observed at the cell surface, suggesting an alteration in the traffic between the EEs and the PM when both GGA adaptors were missing. Finally, 70% of the cells lacking exomer and both GGAs exhibited 9.5 ± 2.3 GFP-Syb1 dots, while the remaining 30% of the cells exhibited 5.1 ± 1 dots that were heterogeneous in size, with 1–2 of them being larger than those observed in the other strains (arrowheads in Figure 4F). Similar results were obtained when the experiment was performed at 36° (data not shown), a temperature that is semirestrictive for the *gga22*Δ *cfr1*Δ mutant, restrictive for the *gga21*Δ *gga22*Δ *cfr1*Δ mutant, and permissive for the rest of the strains (Figure 4B). These results suggested a degree of functional collaboration between exomer and GGAs in some aspect of vesicular trafficking related to the EEs. However, this pattern of GFP-Syb1 localization was different from that exhibited by the *apm1*Δ and *apm1*Δ *cfr1*Δ strains (Figure 2F). Together, these results showed that exomer and GGAs collaborated in a functional pathway required for the organization of subcellular compartments, and strongly suggested

that this collaboration is different from the relationship between exomer and AP-1.

Analysis of functional interaction between exomer, AP-2, AP-3, and clathrin

Since endocytosis is a biological process that involves a clathrin adaptor and trafficking through endosomes, this process was evaluated in *cfr1*Δ mutants. First, we analyzed the genetic interaction between *cfr1*$^+$ and genes involved in endocytosis, and we found that *cfr1*$^+$ interacted genetically with the *SLA2* ortholog *end4*$^+$ (Figure 5A). No synthetic growth defect was found when exomer was deleted in an *apl3*Δ mutant, which lacks the AP-2 α subunit *apl3*$^+$ (Figure 5B). When FM4-64 uptake was evaluated, no delay was detected in the *cfr1*Δ strain (Figure S7). Additionally, according to staining with CDCFDA and FM4-64, vacuole number/morphology were not apparently altered in exomer mutants (Figure 2J, Figure 4D, and Figure S7). These results suggested that if exomer plays a role in the endocytic route, this role must be minor. Following on with the analysis of the relationship between exomer and AP-type adaptors, the existence of genetic interaction between *cfr1*$^+$ and *apm3*$^+$ was investigated. Apm3 is the μ subunit of the AP-3 complex, an adaptor that mediates direct traffic from the Golgi to the vacuoles; in yeast, physical association between AP-3 and clathrin has not been detected. Neither the *apm3*Δ nor the *apm3*Δ *cfr1*Δ strains were thermosensitive (Figure 5C). Finally, the existence of genetic interaction between exomer and clathrin was examined. The *clc1-232* point mutant was used to perform the analysis because the *clc1*Δ mutant is lethal unless cultivated with an osmotic stabilizer (de León *et al.* 2013, 2016). *clc1-232* exhibits synthetic growth defects when combined with *apl3*Δ, *apm1*Δ, and *gga22*Δ mutations (de León *et al.* 2016 and Figure 5D). Similarly, growth of a *clc1-232* *cfr1*Δ strain was less efficient than that of *clc1-232*, showing genetic interaction between *clc1*$^+$ and *cfr1*$^+$ (Figure 5D).

All the results described above showed that exomer is functionally related to several proteins involved in protein trafficking from/to endosomes, and suggested that it might participate in more than one of these routes. Moreover, when Cfr1 distribution was analyzed by subcellular fractionation, it was found that Cfr1-RFP distribution was different from that of Sec72-GFP (Figure 5E and Figure S8). While most of the protein cofractionated with the TGN/EE marker, a part of the protein was reproducibly detected in lighter fractions. This result suggested that a part of exomer complexes might be present in membranes devoid of Sec72, participating in different trafficking routes.

Cfr1 and clathrin adaptors are present in the same complexes

Co-immunoprecipitation experiments were performed to analyze whether Cfr1 interacted physically with clathrin adaptors. We found that Cfr1 was present in immunoprecipitates containing Apm1 (the AP-1 μ subunit), Apm4 (the AP-2 μ subunit), and Gga22 (Figure 6, A–C), but not in immunoprecipitates containing Apm3 (the AP-3 μ subunit. Figure 6D). Similar to the results described in *S. cerevisiae* (Sanchatjate and Schekman 2006; Trautwein *et al.* 2006), we did not detect Cfr1 in Clc1 immunoprecipitates (Figure 6E). Co-immunoprecipitation between Cfr1 and the COPI-subunit Sec28 (Figure 6F), between Cfr1 and the COPI-associated Rer1 receptor, which interacts physically with Sec28 (Figure 6G), and between Cfr1 and the COPII component Sec24 (data not shown) was not detected. Thus, Cfr1 interacts physically with clathrin-associated adaptor complexes but not with other adaptors and coat components.

Exomer mutants exhibit multiple mild defects

If the role of the *S. pombe* exomer in protein trafficking was general, affecting the intracellular transport of diverse proteins (as suggested by the alteration in Golgi morphology), its disruption would lead to pleiotropic phenotypes. We previously reported that the *cfr1*Δ mutant is slightly defective in cell fusion during mating (Cartagena-Lirola *et al.* 2006). Additionally, partial sensitivity to Caspofungin (Figure 2B) suggested a role in cell wall synthesis, which was in agreement with genetic interaction between *cfr1*$^+$ and *cps1/bgs1*$^+$ at high temperature and in the presence of Caspofungin (Figure S1). Furthermore, cell wall composition analyses showed that *cfr1*Δ, *bch1*Δ, and *bch1*Δ *cfr1*Δ strains exhibited a reduced amount of β(1,3)-glucan that was compensated by an increase in the amount of α-glucan (Figure 7A), as described for other strains defective in β(1,3)-glucan synthesis (Ribas *et al.* 1991). Exomer mutants were also sensitive to KCl (Figure 7B), a sensitivity that was accompanied by a defect in septum formation and cell separation (Figure 7C). Finally, *cfr1*Δ was slightly sensitive to high temperature, DTT, tunicamycin, and diverse ions, slightly resistant to some ions, and had reduced growth in minimal medium (Figure 7D). In summary, *S. pombe* exomer mutants exhibited a plethora of mild phenotypes. Thus, although budding and fission yeast exomer exerts a function in vesicle trafficking routes involving TGN/EEs, this function might be more cargo-specific in *S. cerevisiae*.

Discussion

The S. pombe exomer

We have undertaken the study of *S. pombe* proteins similar to exomer components with the aim of complementing the existing knowledge of this adaptor complex. Analysis of Cfr1 and Bch1 has shown that they form a complex that exhibits the basic characteristics of an exomer; *i.e.*, it localizes at internal organelles in an Arf1-dependent manner, and its localization and function is driven by the FBE module (Martin-Garcia *et al.* 2011; Paczkowski *et al.* 2012; this work). Cfr1 is present at organelles that bear Sec72 and can be counterstained with FM4-64. Therefore, similar to budding yeast, this complex localizes at the TGN/EEs, and it is difficult to determine whether it acts at the late Golgi,

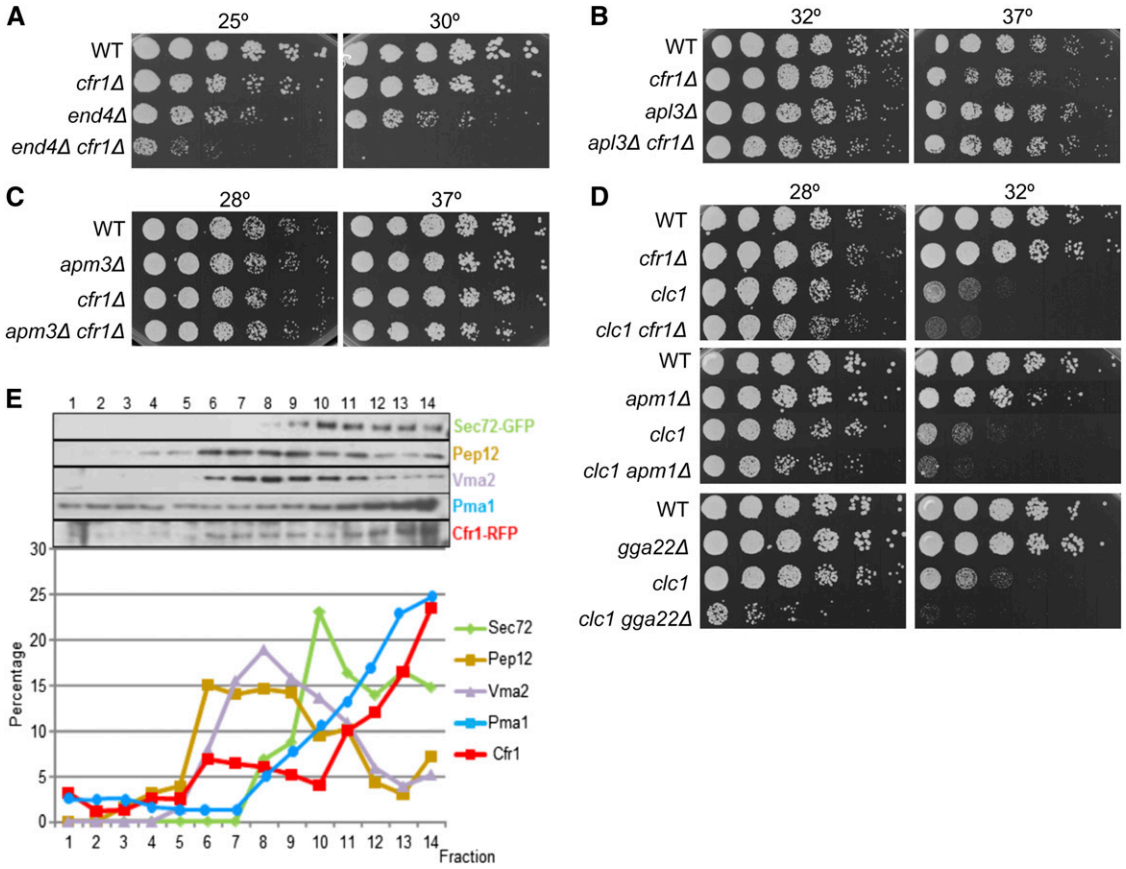

Figure 5 Functional interaction between exomer and other proteins involved in trafficking through endosomes. (A) Cells were spotted onto YES and incubated for 5 days at 25° and for 2 days at 30°. (B–D) The same as in (A), but plates were incubated at the indicated temperatures for 2 days. (E) Cfr1 subcellular distribution. Cell extracts from a strain bearing Cfr1-RFP were centrifuged to equilibrium on mini-step sucrose gradients. Fractions were collected from the lighter to the heavier ones and analyzed by western blot using anti-GFP (Sec72, TGN/EE), anti-Pep12 (PVC), anti-Vma2 (vacuole), anti-RFP and anti-Pma1 (PM) antibodies (upper panel). For each marker, the relative amount in each fraction with respect to its total amount was estimated (lower panel). EE, early endosomes; PM, plasma membrane; PVC, prevacuolar compartment; RFP, red fluorescent protein; TGN, *trans*-Golgi network; WT, wild-type; YES, 0.5% yeast extract, 3% glucose, 225 mg/l adenine, histidine, leucine, uracil, and lysine hydrochloride, and 2% agar.

TGN, EEs, or at all of these organelles. This situation exists because these compartments undergo progressive maturation and continuous fission and fusion events that cause the boundaries between them to be ill-defined, and because the trafficking routes where these organelles participate are complex and interconnected (Lemmon and Traub 2000; Huotari and Helenius 2011; Scott *et al.* 2014).

Golgi organization was slightly altered in *S. pombe* exomer mutants. Aberrant Golgi morphology has been observed under conditions that alter ER to Golgi traffic and traffic through and from the Golgi, probably because of a disequilibrium between protein and lipid input and output ratios (Ward *et al.* 2001; Bhave *et al.* 2014; Papanikou *et al.* 2015). We have found physical and functional interaction between exomer and AP-1, but not between exomer and COPI and COPII. Thus, the most plausible explanation for this phenotype would be that *S. pombe* exomer plays a role in anterograde protein trafficking from the Golgi. However, the aberrant Golgi stacks would still be able to promote delivery of glucan synthases quite effectively. Also, secretion of acid phosphatase is efficient in exomer mutants (results not shown). Nevertheless, although the role of COPI in vesicle trafficking is well-established, COPI-deficient *S. cerevisiae* mutants exhibit aberrant Golgi apparatuses able to promote secretion to almost WT levels (Papanikou *et al.* 2015); thus, the fact that secretion is efficient in *S. pombe* exomer mutants does not necessarily imply that the role of exomer in protein trafficking is not relevant.

Exomer collaborates with clathrin adaptors in several trafficking steps

In *S. cerevisiae*, Chs3 cycles between the TGN and EEs in an AP-1- and exomer-dependent manner (Ziman *et al.* 1996, 1998; Valdivia *et al.* 2002). In the absence of exomer, this enzyme is retained at the TGN/EEs, while in the absence of both adaptors Chs3 is redirected to the cell surface (Valdivia *et al.* 2002). According to fluorescence microscopy, deficiency of *S. pombe* AP-1 results in a partial retention of glucan synthases inside the cells (Yu *et al.* 2012; this work). This alteration in the traffic through the TGN/EEs is accompanied by the accumulation of post-Golgi vesicles when the *apm1Δ* strain is incubated at 37° (Kita *et al.* 2004). We found that

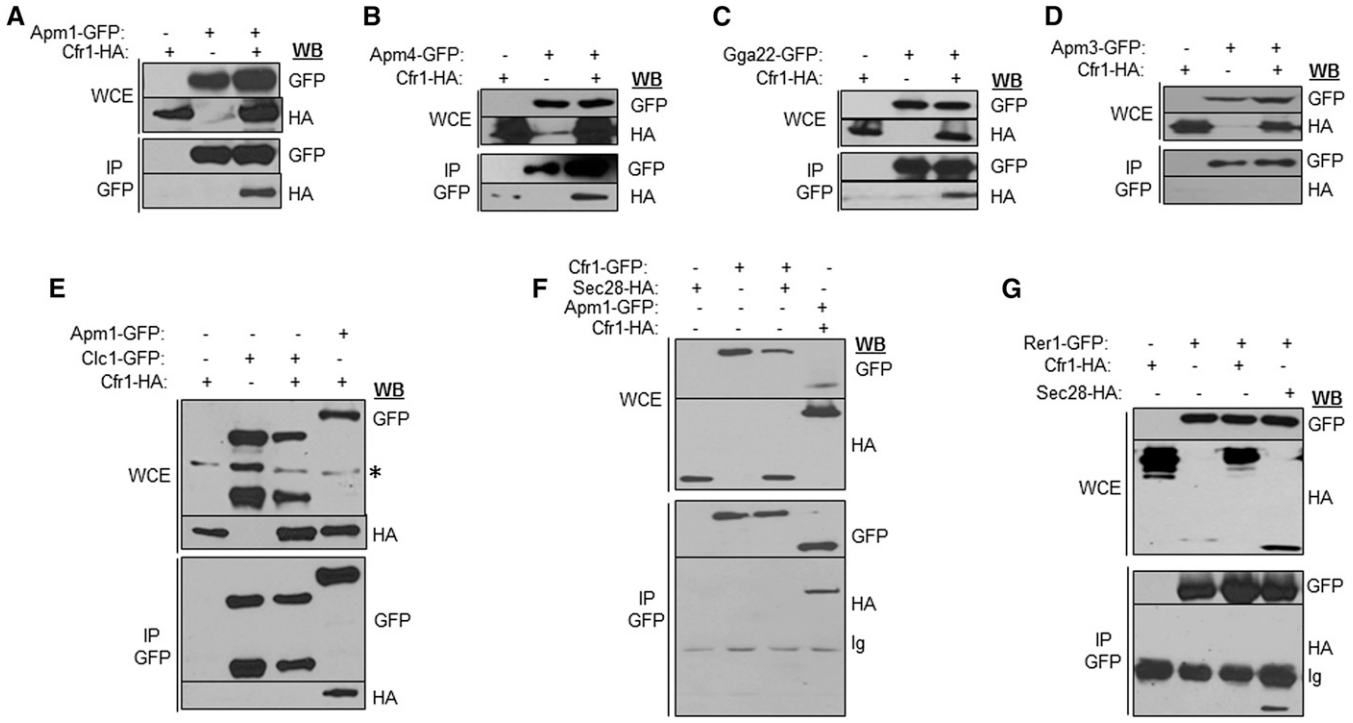

Figure 6 Physical interaction between Cfr1 and clathrin adaptors. (A–D) Analysis of co-immunoprecipitation between Cfr1-HA and GFP-tagged subunits of Assembly Polypeptide (AP) complexes. In all cases, cell extracts from strains bearing each and/or both tagged proteins were analyzed by western blot (WB) using anti-GFP or anti-HA monoclonal antibodies before (WCE, whole-cell extracts) or after immunoprecipitation (IP) with a polyclonal anti-GFP antibody. (E) The same as in (A–D) but co-immunoprecipitation between Cfr1-HA and the clathrin light chain (Clc1-GFP) was analyzed; co-immunoprecipitation between Cfr1-HA and Apm1-GFP was included as a positive control. (F) Analysis of co-immunoprecipitation between Cfr1-GFP and the COPI component Sec28-HA; a strain bearing Cfr1-HA and Apm1-GFP was included as a positive control. (G) Analysis of co-immunoprecipitation between Cfr1-HA and the COPI-associated receptor Rer1-GFP; a strain bearing Sec28-HA and Rer1-GFP was included as a positive control. Ig, Immunoglobulin.

simultaneous elimination of AP-1 and exomer leads to an enhancement of all the *apm1*Δ phenotypes. Thus, the *apm1*Δ *cfr1*Δ strain incubated at 32° exhibits stronger defects than *apm1*Δ in the morphology and organization of the TGN/EEs/vacuoles, the trafficking of glucan synthases, and cell growth. These results showed that both adaptors collaborate in the same trafficking route, where AP-1 plays the most relevant role. Thus, in budding and fission yeast, exomer and AP-1 might participate in the transport of proteins from the TGN/EE to the PM, although the relevance of each adaptor in this process seems to be organism-specific (summarized in Figure 8). According to the data available, in *S. cerevisiae*, exomer is required for anterograde trafficking from the TGN/EE to the PM, while AP-1 is mostly involved in EE to TGN retrograde trafficking. In *S. pombe*, AP-1 plays an important role in the anterograde route, and exomer would collaborate with AP-1 in this trafficking.

GGAs are required for transport from the Golgi to the PVC/vacuole in yeast and mammals, although it is not clear whether they act at the Golgi, TGN, and/or EEs. In *S. cerevisiae*, they are required for Chs3 retention at the TGN/EEs in the absence of exomer, and GGA deletion leads to a defect in the localization of the synaptobrevin-like Snc1 at the PM, showing an alteration in the functionality of EEs (Black and Pelham 2000; Boman *et al.* 2000, 2002; Costaguta *et al.* 2001; He *et al.* 2005; Copic *et al.* 2007; Daboussi *et al.* 2012; Hirst *et al.* 2012). We have detected colocalization between Syb1 and Gga22 (data not shown), and have observed an alteration in GFP-Syb1 localization in *gga21*Δ *gga22*Δ cells, suggesting a role of *S. pombe* GGAs in trafficking through the TGN/EEs. Alteration in the distribution of Syb1 was aggravated by exomer deletion in the *gga21*Δ *gga2*Δ background. Additionally, the triple *gga21*Δ *gga22*Δ *cfr1*Δ mutant exhibited enhanced defects in Cpy1 trafficking, the distribution of the PI3P-binding probe FYVE(EEA1), the morphology/organization of vacuoles, and tolerance to high temperature. Thus, exomer deletion enhances all the phenotypes observed in the *gga21*Δ *gga22*Δ double-mutant. We have not detected colocalization between exomer and either FYVE(EEA1) or Pep12. This negative result does not completely rule out the presence of exomer at the PVC/vacuole, because adaptors accumulate at the membranes producing the vesicles. Nevertheless, the most plausible explanation for phenotype enhancement would be the combination of multiple defects at the TGN/EEs and/or the PVC/vacuoles due to the simultaneous deletion of exomer and GGAs, which would result in a reduced efficiency in trafficking through these organelles.

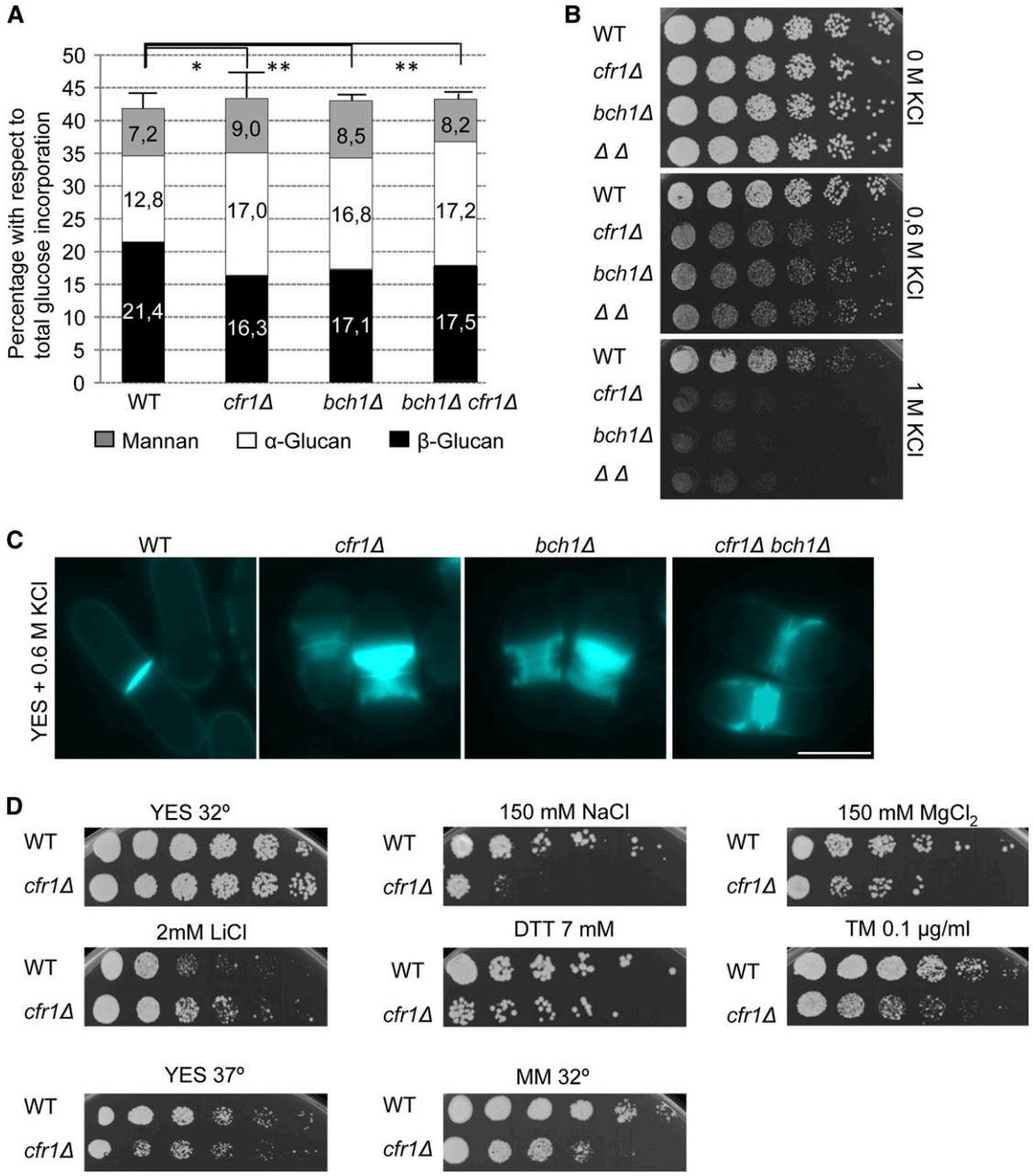

Figure 7 *cfr1*Δ cells exhibit pleiotropic phenotypes. (A) Cell wall analysis of the indicated strains. Bars represent the percentage of incorporation of radioactivity into cell wall polysaccharides of cultures grown in YES medium in the presence of ^{14}C-glucose; values are given as numbers in each bar. The experiment was performed a minimum of five times with duplicates. The mean and SD relative to the total glucose incorporated to the cell wall of each strain are shown. The statistical significance of the difference in β(1,3)-glucan between the mutant strains and the wild-type is shown. (B) Cells were spotted onto YES plates supplemented with the indicated amounts of KCl and incubated at 32° for 2 days. (C) Cells were incubated in YES with 0.6 M KCl for 16 hr at 25°, stained with Calcofluor to allow *in vivo* visualization of the cell wall, and photographed under a conventional fluorescence microscope. The septal area of representative cells is shown. Bar, 10 μm. (D) WT and *cfr1*Δ cells were spotted onto YES plates and YES plates supplemented with the indicated compounds and incubated at 32° for 2 days, spotted onto YES plates and incubated at 37° for 2 days (lower left panel), or spotted onto minimal medium and incubated at 32° for 3 days (lower right panel). WT, wild-type; YES, 0.5% yeast extract, 3% glucose, 225 mg/l adenine, histidine, leucine, uracil, and lysine hydrochloride, and 2% agar.

Therefore, while in budding yeast the effect of eliminating exomer has a drastic effect in the transport of certain cargoes from the TGN/EEs to the PM, our results show that eliminating *S. pombe* exomer has an impact on several trafficking routes. In this organism, exomer would collaborate with AP-1 in protein trafficking from the TGN/EEs to the cell surface and with GGAs in protein trafficking from the TGN/EEs to the vacuole (Figure 8). In these routes, AP-1 and GGA adaptors would play the most relevant roles, while the role of exomer would be minor.

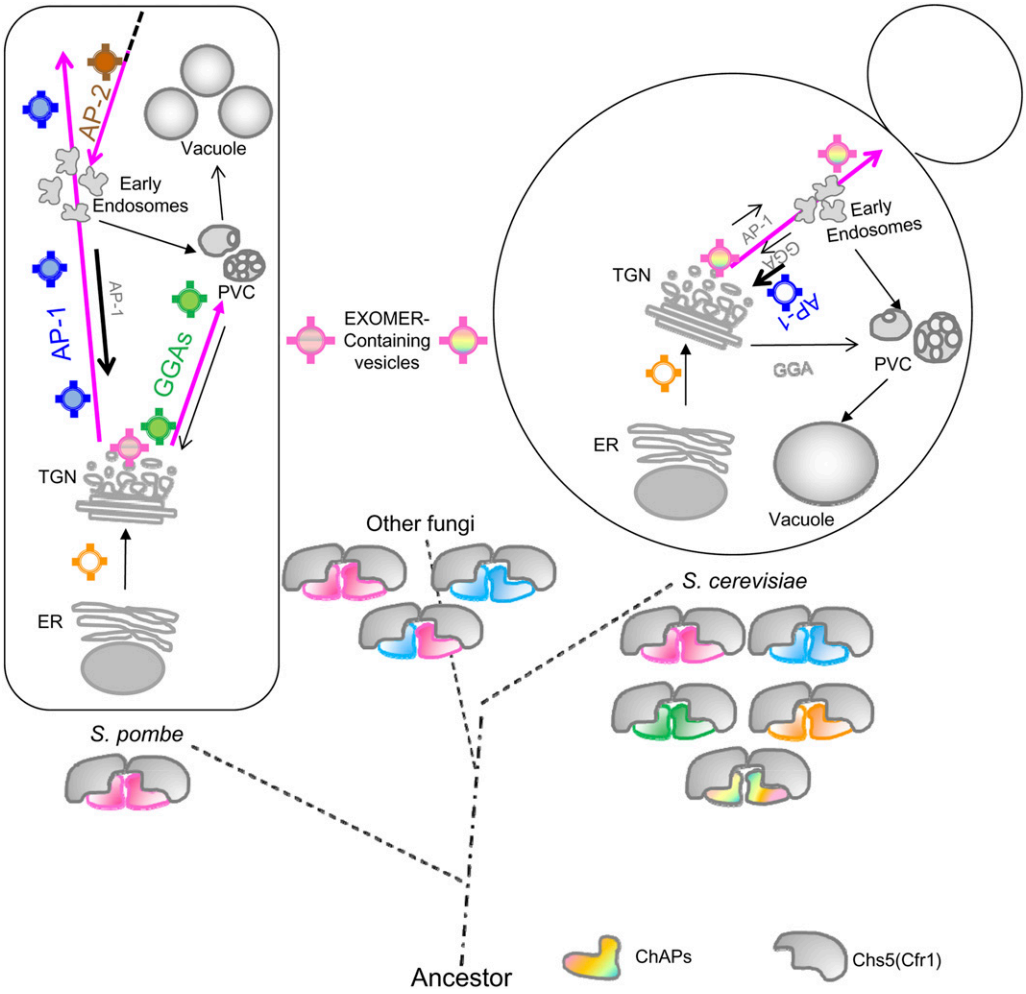

Figure 8 Exomer in *S. pombe* and *S. cerevisiae*. Pink arrows denote the *S. pombe* and *S. cerevisiae* trafficking routes altered in exomer-defective mutants. In fission yeast, exomer is observed at TGN/EEs, interacts physically with Apm1, and collaborates with AP-1 in protein trafficking from the TGN/EEs to the plasma membrane. This collaboration would be required for organelle integrity. Additionally, exomer interacts physically with AP-2 and might participate in a postinternalization step of endocytosis. Exomer also interacts physically with Gga22, and plays a minor role in protein trafficking from the TGN/EEs to the prevacuolar compartment (PVC), where it collaborates with GGA adaptors, which play a major role in this route. This collaboration ensures integrity of the PVC/vacuole compartments. *S. pombe* bears two exomer components, a Chs5-related protein (Cfr1) and one single ChAP (Bch1). Assuming that *S. pombe* exomer would have the same structure described in budding yeast (Paczkowski and Fromme 2014), the complex would be a heterotetramer composed by two Cfr1 and two Bch1 molecules. Exomer would have evolved to originate 2-ChAP and 4-ChAP complexes in different fungi (Roncero *et al.* 2016). In *S. cerevisiae*, the presence of four ChAPs would have allowed a functional specialization of these proteins into the complex, and the recognition of a subset of specific transmembrane cargoes. In budding yeast, exomer is essential for the anterograde transport of these cargoes from the TGN to the plasma membrane through early endosomes, such that cargoes are retained at these organelles in exomer mutants, while in this organism AP-1 is required for retrograde transport from endosomes to the TGN. AP, Assembly Polypeptide; ChAP, Chs5p-Arf1p-binding Protein; EE, early endosomes; ER, endoplasmic reticulum; GGA, Golgi-localized, gamma-adaptin ear domain homology, ARF-binding; MVB, multivesicular body; PM, plasma membrane; PVC, prevacuolar compartment; TGN, *trans*-Golgi network.

cfr1$^+$ exhibits genetic interaction with *end4*$^+$, suggesting a possible exomer role in endocytosis. Although the efficient FM4-64 uptake in *cfr1*Δ does not solely contradict this hypothesis because mutants in clathrin and AP-2 are able to internalize this dye (de León *et al.* 2013, 2016), this observation, together with the fact that Cfr1 is not observed at the PM (Figure 1), suggests that this function might be exerted after cargo internalization. It is possible that AP-2 contacts exomer at endosomes. A requirement for this hypothesis would be that the coated vesicle reaches the endosome and that vesicle uncoating is a sequential process (Trahey and Hay 2010; Semerdjieva 2008) so that clathrin is released from the coat before AP-2 contacts exomer. This hypothesis would be in agreement with the observation that Cfr1 interacts physically with clathrin adaptors but not with clathrin, suggesting that the interaction might take place before clathrin incorporates to the coats or after it dissociates from them.

Evolutionary relationship between exomer and other adaptors

Although Bch1 can be identified in Mycetozoa, red algae, and ciliates, sequences similar to exomer components are mostly represented in fungi that make chitin (Trautwein *et al.* 2006; Roncero *et al.* 2016). However, it is possible that other protein complexes sharing architectural characteristics with exomer may exist and play an equivalent role in protein trafficking from the TGN/EEs to the PM/PVC in other organisms. In agreement with this idea, an ancient protein complex related to COPI and AP adaptors (the TSET complex) has been found in different organisms using structure-based bioinformatics. Similar to the situation with exomer, the penetrance of TSET disruption differs between organisms (Hirst *et al.* 2014). Following the line of thought that architectural similarity might be more relevant than primary sequence, AP-5 subunits share $<$ 10% identity with the subunits of the other

AP complexes, while secondary structure analysis predicts high similarity (Hirst *et al.* 2013). A coevolution of adaptor complexes with the endomembrane system has been proposed such that AP-4 and AP-5 would have evolved from the common ancestor after Golgi appearance (Hirst *et al.* 2011). Similar to AP-4 and AP-5, exomer does not bind clathrin (Sanchatjate and Schekman 2006; Trautwein *et al.* 2006; this work). AP-4 and AP-5 are required for trafficking between the TGN and the PM and for the integrity of the endosomal system (Hirst *et al.* 2011, 2013), the same functions we have found for the *S. pombe* exomer. Neither AP-4 nor AP-5 is present in yeasts; thus, it is possible that in these organisms the function of these adaptors would have been undertaken by exomer at some point in time between the origin of the Golgi and its specialization into the TGN.

As our results show that exomer from distantly-related organisms participates in protein trafficking through the TGN/EEs, what would the conserved exomer function be? Assuming that the *S. pombe* exomer is closer to the ancient complex because it contains a single ChAP, and taking into account the fact that eliminating exomer in this organism produces diverse mild phenotypes, our results suggest that originally this protein complex played a fine-tuning role in trafficking between the TGN/EEs and the PM/PVC, acting in collaboration with other adaptors. Exomer might function as an auxiliary protein complex that would contribute to the efficient functionality of other adaptors. A mutually nonexclusive hypothesis would be that exomer function was required for the establishment of alternative routes in the absence of Apm1 and GGAs, such that partial trafficking from the TGN/EEs to the cell surface and to the vacuoles would take place. Eliminating exomer would not allow these alternative routes to be opened, hampering traffic and leading to the enhancement of specific phenotypes. A general function of exomer in protein trafficking would affect all transport routes, including the alternative pathways. Thus, exomer would participate in a fine-tuning or safety mechanism whose function was relevant in the absence of the main adaptor complexes and under stress conditions. In *S. pombe*, only the basic characteristics of exomer would have been conserved; in *S. cerevisiae*, the ancient whole-genome duplication (Wolfe and Shields 1997) and later duplication events would have led to a more specialized exomer, with multiple ChAPs able to recognize distinct cargoes. Nevertheless, current knowledge is compatible with a general function of budding yeast exomer in trafficking from TGN/EEs to the PM, because it is possible that in exomer mutants the traffic through these organelles is altered in such a way that hampers the anterograde transport of cargoes with certain structural characteristics (which would include, but would not be limited to, the presence of transmembrane domains), while allowing the transport of other proteins. Thus, Fks1 and Skg6 (a protein isolated in a biochemical screen as a potential exomer cargo, Ritz *et al.* 2014) would be able to reach the PM in the absence of exomer, as the glucan synthases are in fission yeast. In a WT strain, the ChAPs might contribute to cargo trafficking from the TGN/EEs by recognizing those particular structural characteristics and/or by promoting the acquisition of a proper cargo conformation such that cargoes can exit the TGN/EEs.

Acknowledgments

We thank E. Keck for language revision. We are indebted to C. Hoffman, T. Kuno, Y. Ohya, S. Oliferenko, P. Pérez, J. C. Ribas, C. Shimoda, K. Takegawa, T. Toda, Y. Toyoshima and the Yeast Genetic Resource Center (http://yeast.lab.nig.ac.jp) for strains and plasmids, C. Castro and C. Anton for help with microscopy, to T. Edreira for help with the statistical analyses, and to Carmen Gutierrez-Gonzalez for technical help. Merck Sharp & Dohme de España, S.A. is acknowledged for the generous gift of Caspofungin. Financial support from the Ministerio de Economía y Competitividad (Spain)/European Union FEDER program (BFU2013-48582-C2-2-P) and from Junta de Castilla y León (SA073U14) to M.-H.V., and from the Swiss National Science Foundation (310030B_163480) to A.S., made this work possible. M.-H.V. was supported by a Junta de Ampliación de Estudios (JAE)-PREDOC Consejo Superior de Investigaciones Científicas (CSIC) fellowship, and F.Y., S.M., N.d.L., and M.-A.C. were supported by Formación de Personal Universitario (FPU) fellowships from the Ministry of Education (Spain).

Literature Cited

Anitei, M., and B. Hoflack, 2011 Exit from the trans-Golgi network: from molecules to mechanisms. Curr. Opin. Cell Biol. 23: 443–451.

Barfield, R. M., J. C. Fromme, and R. Schekman, 2009 The exomer coat complex transports Fus1p to the plasma membrane via a novel plasma membrane sorting signal in yeast. Mol. Biol. Cell 20: 4985–4996.

Barlowe, C. K., and E. A. Miller, 2013 Secretory protein biogenesis and traffic in the early secretory pathway. Genetics 193: 383–410.

Bexiga, M. G., and J. C. Simpson, 2013 Human diseases associated with form and function of the Golgi complex. Int. J. Mol. Sci. 14: 18670–18681.

Bhave, M., E. Papanikou, P. Iyer, K. Pandya, B. K. Jain *et al.*, 2014 Golgi enlargement in Arf-depleted yeast cells is due to altered dynamics of cisternal maturation. J. Cell Sci. 127: 250–257.

Black, M. W., and H. R. Pelham, 2000 A selective transport route from Golgi to late endosomes that requires the yeast GGA proteins. J. Cell Biol. 151: 587–600.

Boman, A. L., C. Zhang, X. Zhu, and R. A. Kahn, 2000 A family of ADP-ribosylation factor effectors that can alter membrane transport through the trans-Golgi. Mol. Biol. Cell 11: 1241–1255.

Boman, A. L., P. D. Salo, M. J. Hauglund, N. L. Strand, S. J. Rensink *et al.*, 2002 ADP-ribosylation factor (ARF) interaction is not sufficient for yeast GGA protein function or localization. Mol. Biol. Cell 13: 3078–3095.

Bonifacino, J. S., 2014 Adaptor proteins involved in polarized sorting. J. Cell Biol. 204: 7–17.

Burd, C. G., and S. D. Emr, 1998 Phosphatidylinositol(3)-phosphate signaling mediated by specific binding to RING FYVE domains. Mol. Cell 2: 157–162.

Cartagena-Lirola, H., A. Duran, and M. H. Valdivieso, 2006 The *Schizosaccharomyces pombe cfr1*$^{+}$ gene participates in mating through a new pathway that is independent of *fus1*$^{+}$. Yeast 23: 375–388.

Copic, A., T. L. Starr, and R. Schekman, 2007 Ent3p and Ent5p exhibit cargo-specific functions in trafficking proteins between the trans-Golgi network and the endosomes in yeast. Mol. Biol. Cell 18: 1803–1815.

Costaguta, G., C. J. Stefan, E. S. Bensen, S. D. Emr, and G. S. Payne, 2001 Yeast Gga coat proteins function with clathrin in Golgi to endosome transport. Mol. Biol. Cell 12: 1885–1896.

Daboussi, L., G. Costaguta, and G. S. Payne, 2012 Phosphoinositide-mediated clathrin adaptor progression at the trans-Golgi network. Nat. Cell Biol. 14: 239–248.

de León, N., M. R. Sharifmoghadam, M. Hoya, M. Á. Curto, C. Doncel *et al.*, 2013 Regulation of cell wall synthesis by the clathrin light chain is essential for viability in *Schizosaccharomyces pombe*. PLoS One 8: e71510.

de León, N., M. Hoya, M. A. Curto, S. Moro, F. Yanguas *et al.*, 2016 The AP-2 complex is required for proper temporal and spatial dynamics of endocytic patches in fission yeast. Mol. Microbiol. 100: 409–424.

De Matteis, M. A., and A. Luini, 2008 Exiting the Golgi complex. Nat. Rev. Mol. Cell Biol. 9: 273–284.

Doray, B., P. Ghosh, J. Griffith, H. J. Geuze, and S. Kornfeld, 2002 Cooperation of GGAs and AP-1 in packaging MPRs at the trans-Golgi network. Science 297: 1700–1703.

Edamatsu, M., and Y. Y. Toyoshima, 2003 Fission yeast synaptobrevin is involved in cytokinesis and cell elongation. Biochem. Biophys. Res. Commun. 301: 641–645.

Fennessy, D., A. Grallert, A. Krapp, A. Cokoja, A. J. Bridge *et al.*, 2014 Extending the *Schizosaccharomyces pombe* molecular genetic toolbox. PLoS One 9: e97683.

Guo, Y., D. W. Sirkis, and R. Schekman, 2014 Protein sorting at the trans-Golgi network. Annu. Rev. Cell Dev. Biol. 30: 169–206.

He, X., F. Li, W. P. Chang, and J. Tang, 2005 GGA proteins mediate the recycling pathway of memapsin 2 (BACE). J. Biol. Chem. 280: 11696–11703.

Hirst, J., L. D. Barlow, G. C. Francisco, D. A. Sahlender, M. N. Seaman *et al.*, 2011 The fifth adaptor protein complex. PLoS Biol. 9: e1001170.

Hirst, J., G. H. Borner, R. Antrobus, A. A. Peden, N. A. Hodson *et al.*, 2012 Distinct and overlapping roles for AP-1 and GGAs revealed by the "knocksideways" system. Curr. Biol. 22: 1711–1716.

Hirst, J., C. Irving, and G. H. Borner, 2013 Adaptor protein complexes AP-4 and AP-5: new players in endosomal trafficking and progressive spastic paraplegia. Traffic 14: 153–164.

Hirst, J., A. Schlacht, J. P. Norcott, D. Traynor, G. Bloomfield *et al.*, 2014 Characterization of TSET, an ancient and widespread membrane trafficking complex. eLife 3: e02866.

Huotari, J., and A. Helenius, 2011 Endosome maturation. EMBO J. 30: 3481–3500.

Huranova, M., G. Muruganandam, M. Weiss, and A. Spang, 2016 Dynamic assembly of the exomer secretory vesicle cargo adaptor subunits. EMBO Rep. 17: 202–219.

Kita, A., R. Sugiura, H. Shoji, Y. He, L. Deng *et al.*, 2004 Loss of Apm1, the micro1 subunit of the clathrin-associated adaptor-protein-1 complex, causes distinct phenotypes and synthetic lethality with calcineurin deletion in fission yeast. Mol. Biol. Cell 15: 2920–2931.

Lemmon, S. K., and L. M. Traub, 2000 Sorting in the endosomal system in yeast and animal cells. Curr. Opin. Cell Biol. 12: 457–466.

Liu, J., H. Wang, and M. K. Balasubramanian, 2000 A checkpoint that monitors cytokinesis in *Schizosaccharomyces pombe*. J. Cell Sci. 113(Pt 7): 1223–1230.

Martin-Garcia, R., A. Duran, and M. H. Valdivieso, 2003 In *Schizosaccharomyces pombe* chs2p has no chitin synthase activity but is related to septum formation. FEBS Lett. 549: 176–180.

Martin-Garcia, R., N. de León, M. R. Sharifmoghadam, M. A. Curto, M. Hoya *et al.*, 2011 The FN3 and BRCT motifs in the exomer component Chs5p define a conserved module that is necessary and sufficient for its function. Cell. Mol. Life Sci. 68: 2907–2917.

Meyer, C., D. Zizioli, S. Lausmann, E. L. Eskelinen, J. Hamann *et al.*, 2000 mu1A-adaptin-deficient mice: lethality, loss of AP-1 binding and rerouting of mannose 6-phosphate receptors. EMBO J. 19: 2193–2203.

Moreno, S., A. Klar, and P. Nurse, 1991 Molecular genetic analysis of fission yeast *Schizosaccharomyces pombe*. Methods Enzymol. 194: 795–823.

Paczkowski, J. E., and J. C. Fromme, 2014 Structural basis for membrane binding and remodeling by the exomer secretory vesicle cargo adaptor. Dev. Cell 30: 610–624.

Paczkowski, J. E., B. C. Richardson, A. M. Strassner, and J. C. Fromme, 2012 The exomer cargo adaptor structure reveals a novel GTPase-binding domain. EMBO J. 31: 4191–4203.

Papanikou, E., K. J. Day, J. Austin, and B. S. Glick, 2015 COPI selectively drives maturation of the early Golgi. eLife 4: e13232.

Perez, P., and J. C. Ribas, 2004 Cell wall analysis. Methods 33: 245–251.

Reyes, A., M. Sanz, A. Duran, and C. Roncero, 2007 Chitin synthase III requires Chs4p-dependent translocation of Chs3p into the plasma membrane. J. Cell Sci. 120: 1998–2009.

Ribas, J. C., M. Diaz, A. Duran, and P. Perez, 1991 Isolation and characterization of *Schizosaccharomyces pombe* mutants defective in cell wall (1,3)β-D-glucan. J. Bacteriol. 173: 3456–3462.

Ritz, A. M., M. Trautwein, F. Grassinger, and A. Spang, 2014 The prion-like domain in the exomer-dependent cargo Pin2 serves as a trans-Golgi retention motif. Cell Rep. 7: 249–260.

Rockenbauch, U., A. M. Ritz, C. Sacristan, C. Roncero, and A. Spang, 2012 The complex interactions of Chs5p, the ChAPs, and the cargo Chs3p. Mol. Biol. Cell 23: 4402–4415.

Roncero, C., A. Sanchez-Diaz, and M. H. Valdivieso, 2016 Chitin synthesis and fungal cell morphogenesis, *The Mycota*, edited by K. Esser, and D. Hoffmeister. Springer, Heidelberg.

Sambrook, J., and D. W. Russell, 2001 Molecular Cloning: A *L*aboratory *M*anual. Cold Spring Harbor Laboratory Press, Cold Spring Harbor, NeY.

Sanchatjate, S., and R. Schekman, 2006 Chs5/6 complex: a multiprotein complex that interacts with and conveys chitin synthase III from the trans-Golgi network to the cell surface. Mol. Biol. Cell 17: 4157–4166.

Sanchez-Mir, L., A. Franco, R. Martin-Garcia, M. Madrid, J. Vicente-Soler *et al.*, 2014 Rho2 palmitoylation is required for plasma membrane localization and proper signaling to the fission yeast cell integrity mitogen- activated protein kinase pathway. Mol. Cell. Biol. 34: 2745–2759.

Santos, B., and M. Snyder, 1997 Targeting of chitin synthase 3 to polarized growth sites in yeast requires Chs5p and Myo2p. J. Cell Biol. 136: 95–110.

Santos, B., and M. Snyder, 2003 Specific protein targeting during cell differentiation: polarized localization of Fus1p during mating depends on Chs5p in *Saccharomyces cerevisiae*. Eukaryot. Cell 2: 821–825.

Santos, B., A. Durán, and M. H. Valdivieso, 1997 *CHS5*, a gene involved in chitin synthesis and mating in *Saccharomyces cerevisiae*. Mol. Cell. Biol. 17: 2485–2496.

Scott, C. C., F. Vacca, and J. Gruenberg, 2014 Endosome maturation, transport and functions. Semin. Cell Dev. Biol. 31: 2–10.

Sharifmoghadam, M. R., and M. H. Valdivieso, 2009 The fission yeast SEL1 domain protein Cfh3p: a novel regulator of the glucan synthase Bgs1p whose function is more relevant under stress conditions. J. Biol. Chem. 284: 11070–11079.

Semerdjieva, S., B. Shortt, E. Maxwell, S. Singh, P. Fonarev *et al.*, 2008 Coordinated regulation of AP2 uncoating from clathrin-coated vesicles by rab5 and hRME-6. J. Cell Biol. 183: 499–511.

Spang, A., 2015 The road not taken: less traveled roads from the TGN to the plasma membrane. Membranes (Basel) 5: 84–98.

Tang, B. L., 2009 Neuronal protein trafficking associated with Alzheimer disease: from APP and BACE1 to glutamate receptors. Cell Adhes. Migr. 3: 118–128.

Trahey, M., and J. C. Hay, 2010 Transport vesicle uncoating: it's later than you think. F1000 Biol. Rep. 2: 47.

Trautwein, M., C. Schindler, R. Gauss, J. Dengjel, E. Hartmann *et al.*, 2006 Arf1p, Chs5p and the ChAPs are required for export of specialized cargo from the Golgi. EMBO J. 25: 943–954.

Valdez-Taubas, J., and H. R. Pelham, 2003 Slow diffusion of proteins in the yeast plasma membrane allows polarity to be maintained by endocytic cycling. Curr. Biol. 13: 1636–1640.

Valdivia, R. H., D. Baggott, J. S. Chuang, and R. W. Schekman, 2002 The yeast clathrin adaptor protein complex 1 is required for the efficient retention of a subset of late Golgi membrane proteins. Dev. Cell 2: 283–294.

Vo, T. V., J. Das, M. J. Meyer, N. A. Cordero, N. Akturk *et al.*, 2016 A proteome-wide fission yeast interactome reveals network evolution principles from yeasts to human. Cell 164: 310–323.

Wakana, Y., J. van Galen, F. Meissner, M. Scarpa, R. S. Polishchuk *et al.*, 2012 A new class of carriers that transport selective cargo from the trans Golgi network to the cell surface. EMBO J. 31: 3976–3990.

Wang, C. W., S. Hamamoto, L. Orci, and R. Schekman, 2006 Exomer: a coat complex for transport of select membrane proteins from the trans-Golgi network to the plasma membrane in yeast. J. Cell Biol. 174: 973–983.

Ward, T. H., R. S. Polishchuk, S. Caplan, K. Hirschberg, and J. Lippincott-Schwartz, 2001 Maintenance of Golgi structure and function depends on the integrity of ER export. J. Cell Biol. 155: 557–570.

Wolfe, K. H., and D. C. Shields, 1997 Molecular evidence for an ancient duplication of the entire yeast genome. Nature 387: 708–713.

Yu, Y., A. Kita, M. Udo, Y. Katayama, M. Shintani *et al.*, 2012 Sip1, a conserved AP-1 accessory protein, is important for Golgi/endosome trafficking in fission yeast. PLoS One 7: e45324.

Ziman, M., J. S. Chuang, and R. W. Schekman, 1996 Chs1p and Chs3p, two proteins involved in chitin synthesis, populate a compartment of the *Saccharomyces cerevisiae* endocytic pathway. Mol. Biol. Cell 7: 1909–1919.

Ziman, M., J. S. Chuang, M. Tsung, S. Hamamoto, and R. Schekman, 1998 Chs6p-dependent anterograde transport of Chs3p from the chitosome to the plasma membrane in *Saccharomyces cerevisiae*. Mol. Biol. Cell 9: 1565–1576.

Communicating editor: M. D. Rose